Skeletal Radiology (2019) 48:653–676
https://doi.org/10.1007/s00256-018-3107-1

REVIEW ARTICLE

Whole-body MRI and pathological findings in adult patients with myopathies

Xavier Tomas[1] · Jose Cesar Milisenda[2] · Ana Isabel Garcia-Diez[1] · Sergio Prieto-Gonzalez[3] · Marie Faruch[4] · Jaime Pomes[1] · Josep Maria Grau-Junyent[2]

Received: 5 July 2018 / Revised: 12 October 2018 / Accepted: 22 October 2018 / Published online: 30 October 2018

Abstract

Magnetic resonance imaging (MRI) is considered the most sensitive and specific imaging technique for the detection of muscle diseases related to myopathies. Since 2008, the use of whole-body MRI (WBMRI) to evaluate myopathies has improved due to technical advances such as rolling table platform and parallel imaging, which enable rapid assessment of the entire musculoskeletal system with high-quality images. WBMRI protocols should include T1-weighted and short-tau inversion recovery (STIR), which provide the basic pulse sequences for studying myopathies, in order to detect fatty infiltration/muscle atrophy and muscle edema, respectively. High signal intensity in T1-weighted images shows chronic disease with fatty infiltration, whereas high signal intensity in STIR indicates an acute stage with muscle edema. Additional sequences such as diffusion-weighted imaging (DWI) can be readily incorporated into routine WBMRI study protocols. Contrast-enhanced sequences have not been done. This article reviews WBMRI as an imaging method to evaluate different myopathies (idiopathic inflammatory, dystrophic, non-dystrophic, metabolic, and channelopathies). WBMRI provides a comprehensive estimate of the total burden with a single study, seeking specific distribution patterns, including clinically silent involvement of muscle areas. Furthermore, WBMRI may help to select the "target muscle area" for biopsy during patient follow-up. It may be also be used to detect related and non-related pathological conditions, such as tumors.

Keywords Biopsy · Muscle · Myopathies · Myositis · Whole-body MRI · Dystrophic myopathies · Congenital myopathies · Metabolic myopathies · Channelopathies

Introduction

Idiopathic inflammatory myopathies (IIMs) are a heterogeneous group of potentially treatable autoimmune muscle diseases, having a significant morbidity and mortality. Myositis-specific antibodies have led to further categorization of IIMs from the traditional polymyositis (PM) versus dermatomyositis (DM), to other entities such as necrotizing autoimmune myopathy (NAM) [1]. Another two subcategories including sporadic inclusion-body myositis (s-IBM) and overlap myositis syndromes (systemic sclerosis being the most common) have also been recognized [2]. Taking into account the potential susceptibility of these diseases to therapy, early and correct diagnosis and a detailed work-up to evaluate therapeutic response are mandatory. On the other hand, other myopathies, or the so-called "non-idiopathic inflammatory myopathies", including dystrophic, congenital, metabolic, and channelopathies, are classified differently since the therapy and prognosis of these diseases are completely different. The aim of this review was to describe the histological and whole-body MRI (WBMRI) patterns of muscle involvement to achieve an early and accurate diagnosis of the type of myopathy. In addition, we describe additional advantages of WBMRI such as its use in "guiding muscle biopsy", monitoring patient follow-up and detecting both related and non-related abnormalities (Table 1).

✉ Xavier Tomas
xtomas61@gmail.com

[1] Department of Radiology (CDIC), Hospital Clinic, Universitat de Barcelona (UB), Villarroel 170, 08036 Barcelona, Spain

[2] Department of Internal Medicine, Hospital Clinic, Universitat de Barcelona (UB) and CIBERER, Villarroel 170, 08036 Barcelona, Spain

[3] Department of Autoimmune Diseases, Hospital Clinic, Universitat de Barcelona (UB), Villarroel 170, 08036 Barcelona, Spain

[4] Department of Radiology, Hopital Purpan, Centre Hospitalier Universitaire (CHU), Place du Docteur Baylac TSA 40031, 31059 Toulouse cedex 9, France

Table 1 Table of contents/outline

Whole-body MRI technique (WBMRI)

Due to its excellent soft tissue contrast, MRI is currently a useful imaging method for studying myopathies [3]. WBMRI has become increasingly important in the last years for assessing the entire musculoskeletal system, including the psoas, intercostal, neck, and muscles of the lower limbs, which are not visualized using standard MRI protocols [4–7]. In our study, all images were acquired using a 1.5-T MR scanner (Aera; Siemens. Erlangen, Germany), and were performed in the axial and coronal plane using T1-weighted turbo spin-echo, STIR sequences and diffusion-weighted imaging (b50-b800DWI). For the whole-body scan, axial slices were made at five contiguous stations. Contrast was not used in any of the patients. The acquisition time was 50–60 min. Institutional review board approval was obtained and written informed consent was waived.

Muscle MRI patterns: Edema, fat replacement, and apparent diffusion coefficient (ADC)

Edema

In the STIR or fat-suppressed T2 sequences, the fat presents a low signal while fluid (edema) and is hyperintense, facilitating visualization of these two processes [8]. STIR is quicker to obtain and more homogeneous than T2 sequence [9]. In the acute stage of the disease, MRI shows muscle edema in most (76–97%) patients suffering idiopathic inflammatory myopathies [10–13], which often, albeit not always, corresponds to abnormalities in electromyography (EMG) and/or creatine kinase (CK) levels. In patients with symptoms suggestive of myopathy but with normal muscle enzyme values, MRI (muscle edema) can provide added value for achieving the diagnosis [14].

Fat replacement

A chronic inflammatory myopathic process can induce several pathologic changes within the muscle, including loss of muscle bulk (atrophy) and fatty involution (fat replacement), producing largely irreversible damage as opposed to disease activity [15]. Fat replacement appears hyperintense on T1-weighted images, while edema appears as a low signal [9]. MRI scoring systems developed to semi-quantitatively evaluate muscle inflammation, muscle volume, and the degree of fat replacement in neuromuscular conditions [16], are often more effective than clinical muscle testing in the evaluation of muscle disease [17, 18]. Most classifications or diagnostic criteria developed for idiopathic inflammatory myopathies exclude MRI as a variable [15, 19, 20], whereas in 2004 other groups such as ENMC consider MRI finding of edema in STIR images as one of the variables [21]. In summary, there is no universally accepted consensus for the scoring and reporting of MRI findings [22].

Diffusion-weighted imaging (DWI), apparent diffusion coefficient (ADC)

Diffusion-weighted imaging (DWI) is a functional MRI technique, the basic principle of which is stochastic Brownian motion or specific diffusion of extra-cellular water molecules within tissues. Diffusion therefore indirectly reflects the histology of tissues (cellularity as well as fibrosis and hemoglobin degradation products). DWI is obtained by out-of-phase spin using a diffusion gradient ("b") with in phase using a second gradient. When diffusion is high, the return to phase is incomplete: spins are out of phase and move and no longer make use of the back in phase gradient. The use of "b" factors varies but is generally high. If b = 0 or low, a T2-weighted image is obtained without a true DWI. Conversely, if the b value is high (for example b = 800), a genuine DWI is obtained beyond the T2 and perfusion image,

generally with poorer spatial resolution and a poorer signal-to-noise ratio. Diffusion-weighted MR images must therefore be visually assessed, comparing the images obtained with a low b value (T2-weighting) with those obtained with a high b value. The difference in signal between these two images is related to water diffusion. Diffusion is represented by a quantitative variable, the apparent diffusion coefficient (ADC), which is the first-line method to assess DWI data [23]. DWI sequences can be readily incorporated into routine MRI study protocols requiring no more than 5 min [24]. Diffusion is increased (elevated ADC compared to normal muscles) in active inflammation due to increased capillary perfusion [25]. Conversely, diffusion is decreased (lower ADC values compared to normal muscles) in the case of fatty degeneration, due to a reduction in water content, being a biomarker of disease progression and response to treatment in myopathies [25, 26]. At present, DWI is the most advanced MRI technique showing clinical benefits in the study of myopathies [15].

Idiopathic inflammatory myopathies (IIMs)

Dermatomyositis (DM)

DM affects children and adults alike, being more common in women and the most common inflammatory myopathy in children. The presentation is usually subacute, with muscle pain weakness and stiffness and purple discoloration of the upper eyelids ("heliotrope"), edema around the eyes, facial erythema, and scaly erythematous papules on the elbows, knuckles, and any of the finger joints, the latter being known as Gottron's sign (Fig. 1). Subcutaneous calcifications are characteristic of DM [2]. In adults, the risk of developing cancer (ovarian, breast, and lung, among others) is increased during the first 3 to 5 years after the onset of DM, with a reported frequency of 15–32%. An annual workup is therefore essential during the first 3 years after disease onset [27, 28]. Although a positron emission tomography-computerized tomography (PET-CT) study as a single imaging technique is recommended in this scenario, WBMRI can help to detect associated malignancies in these patients. In patients with DM, a common MRI finding is edema along the muscle fascia and in the subcutaneous tissue (Fig. 1), which is less commonly seen in patients with polymyositis [29].

Polymyositis (PM)

The diagnosis of PM is achieved by exclusion, and is best defined as a subacute proximal myopathy in adults not presenting a rash, a family history of neuromuscular disease, exposure to myotoxic drugs (e.g., statins, penicillamine, and zidovudine, among others), involvement of facial and extraocular muscles, endocrine disease, or the clinical phenotype of inclusion-body myositis [2]. PM is more common in women and may be associated with malignancy, although the risk of malignancy is lower than in DM. Up to one-third of the cases of PM are associated with a systemic autoimmune disease [2]. DM and PM commonly lead to symmetric involvement of the extremities (Fig. 2), with relative sparing of the distal muscles and those of the body trunk [6, 30, 31]. Edema has been described as "patchy" in DM and "diffuse" in PM [32, 33]. DM frequently involves the quadriceps femoris, whereas PM involves the adductors [34].

Sporadic inclusion body myositis (s-IBM)

s-IBM is a slowly progressive inflammatory and degenerative muscle disease, which is the most common and disabling IIMs in people over 50 years of age [2, 35–41]. Muscle atrophy and fatty degeneration are the predominant findings. Early symptoms include involvement of the distal muscles, especially foot extensors and finger flexors, atrophy of the forearm and quadriceps muscles, mild facial-muscle weakness [2, 36, 39–41] and dysphagia in more than 50% of the patients [41]. The axial muscles may also be affected, resulting in camptocormia syndrome (bending forward of the spine) or head drop [2]. Unlike DM and PM, s-IBM is not associated with malignancy [42]. Disease onset is insidious and develops over a period of years, (fatty replacement being the most striking MRI finding), sometimes asymmetrically (Fig. 3) in 10–44% of the patients [32, 34, 43]. A typical pattern involves the quadriceps muscle (with relative sparing of the rectus femoris), the distal sartorius, severe atrophy of the medial gastrocnemius, the ankle dorsiflexors and the wrist and deep finger flexors, whereas the adductor and abductor muscles of the shoulder and pelvic girdles are relatively spared [44].

Necrotizing autoimmune myopathy (NAM)

NAM accounts for up to 19% of all IIM [45], and may develop alone or following a viral infection, or in association with cancer, systemic autoimmune diseases, or in patients taking statins. For instance, most patients with NAM have antibodies against the signal recognition particle (SRP) or 3-hydroxy-3-methylglutaryl coenzyme A reductase (HMGCR) [46–48]. Regarding statins-related myopathy, in cases showing improvement of myopathy within 4 to 6 weeks after discontinuation of statins treatment, it can be assumed that the etiology is a reversible toxic effect. On the contrary, myopathy continues to worsen after statins withdrawal; MAM must be considered, and a muscle biopsy is mandatory [36, 46–49]. Severe fatty replacement has been found in patients with anti-SRP antibodies, particularly in the hamstrings and adductor magnus [35]. Edema tends to be marked in the vastus lateralis with relative sparing of the vastus intermedius [35, 36]. A recent study of over 666 subjects, including 101 patients with NAM, showed

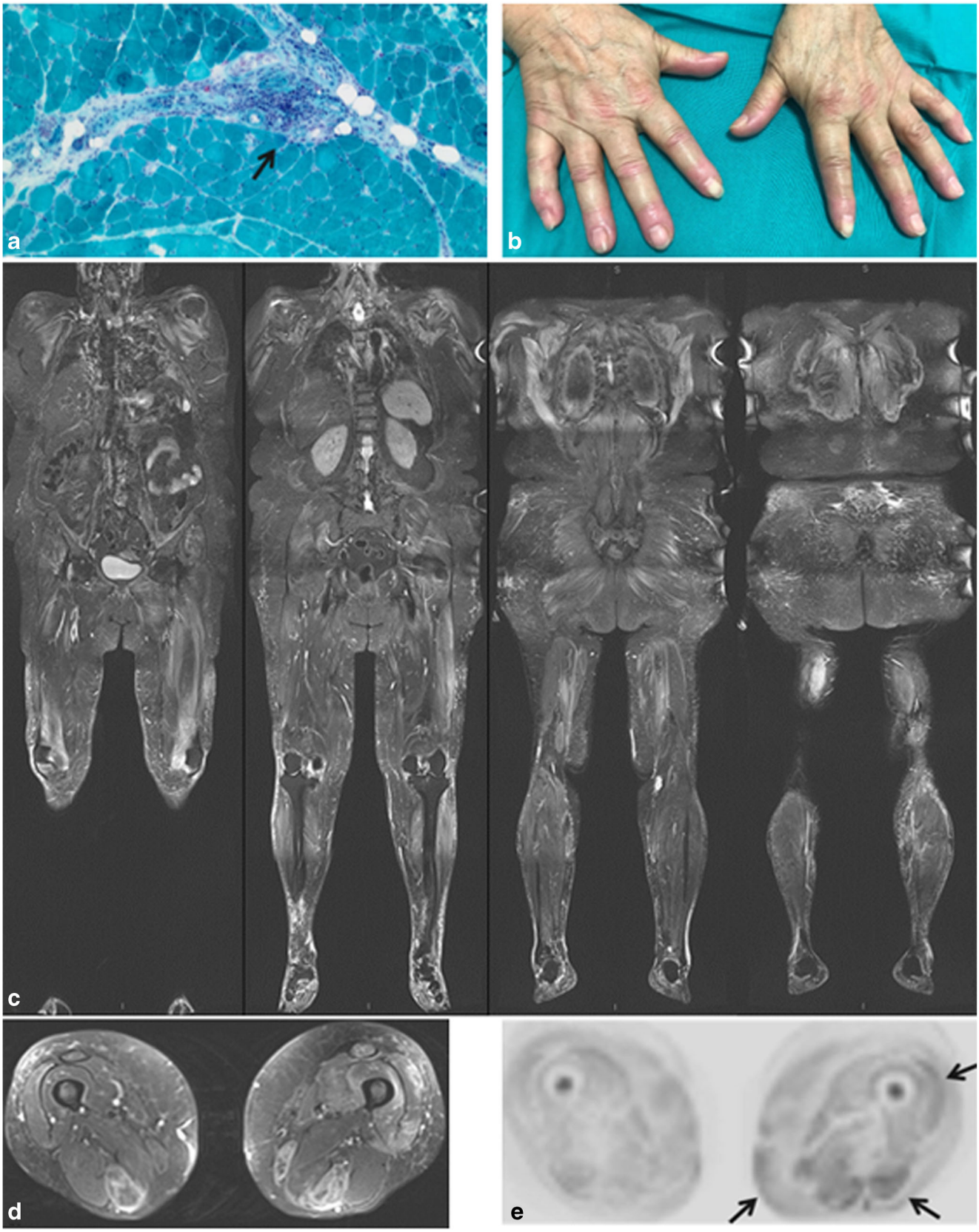
a
b
c
d
e

◀ **Fig. 1** A 75-year-old woman with dermatomyositis. **a** Photomicrographs of the frozen muscle tissue stained with Gomori's trichrome showing perivascular inflammatory cells (arrows) with perifascicular atrophy. **b** Gottron's sign in hands: red, sometimes scaly, papules that erupt on any of the finger joints (in metacarpophalangeal or interphalangeal joints). **c** Coronal STIR-weighted WBMRI shows bilateral symmetrical muscle and fascial edema of the shoulder girdle, thoracic wall and legs, as well as subcutaneous edema of the gluteal area. **d** and **e**, comparative axial STIR-weighted (**d**) and a high-b-value of 800 s/mm^2 DWI WBMRI (**e**) of the thighs showing elevated signal on STIR and DWI (diffusion restriction and "T2-shine-through") of muscles with inflammation respectively (*arrows*)

a higher proportion of thigh muscle edema, atrophy, and fatty infiltration compared with DM or PM [50] (Figs. 4, 5, and 6).

Overlap syndromes

Myositis may be part of the clinical spectrum of other autoimmune diseases such as systemic autoimmune diseases, the most frequent being systemic sclerosis, followed by systemic lupus erythematous (SLE) [14]. The proximal muscles of the upper and lower extremities are the most frequently involved, similar to classical

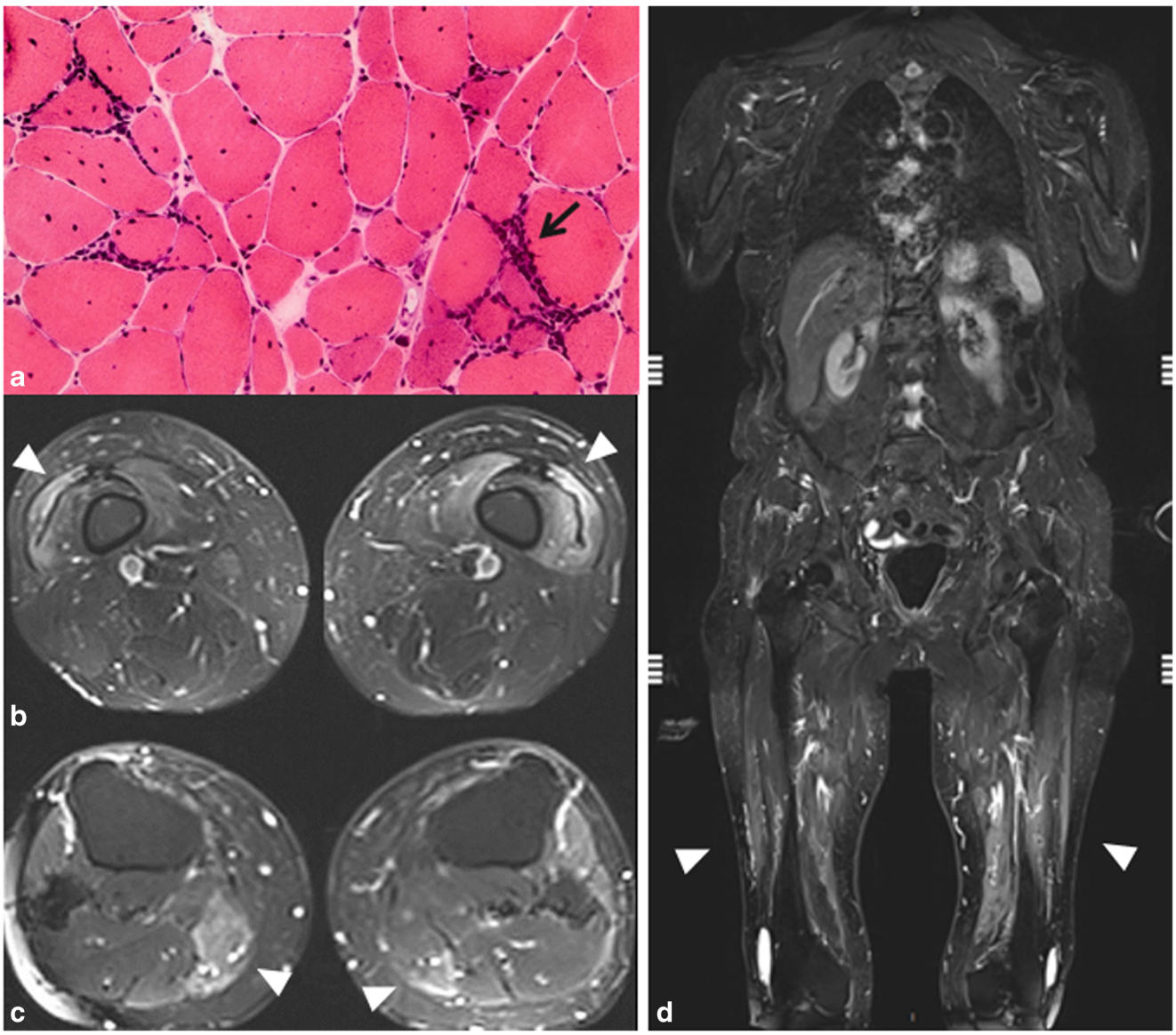

Fig. 2 A 50-year-old woman with polymyositis. **a** Muscle (H&E in frozen tissue) biopsy showing variability in fiber size with an endomysial inflammatory infiltrate (*arrow*) and partial non-necrotic cells invasion. **b**, **c** Axial STIR-weighted WBMRI shows bilateral symmetrical edema (*arrowheads*) of the thighs (**b**) and legs (**c**). In this case, we did not observe the previously reported "diffuse" (vs. patchy) edema or involvement of the adductors (vs. quadriceps) muscles, suggesting that these MRI signs should not be strictly considered. **d** Coronal STIR-weighted WBMRI shows bilateral symmetrical edema of the thighs (*arrowheads*). The shoulder and pelvic girdles were not involved

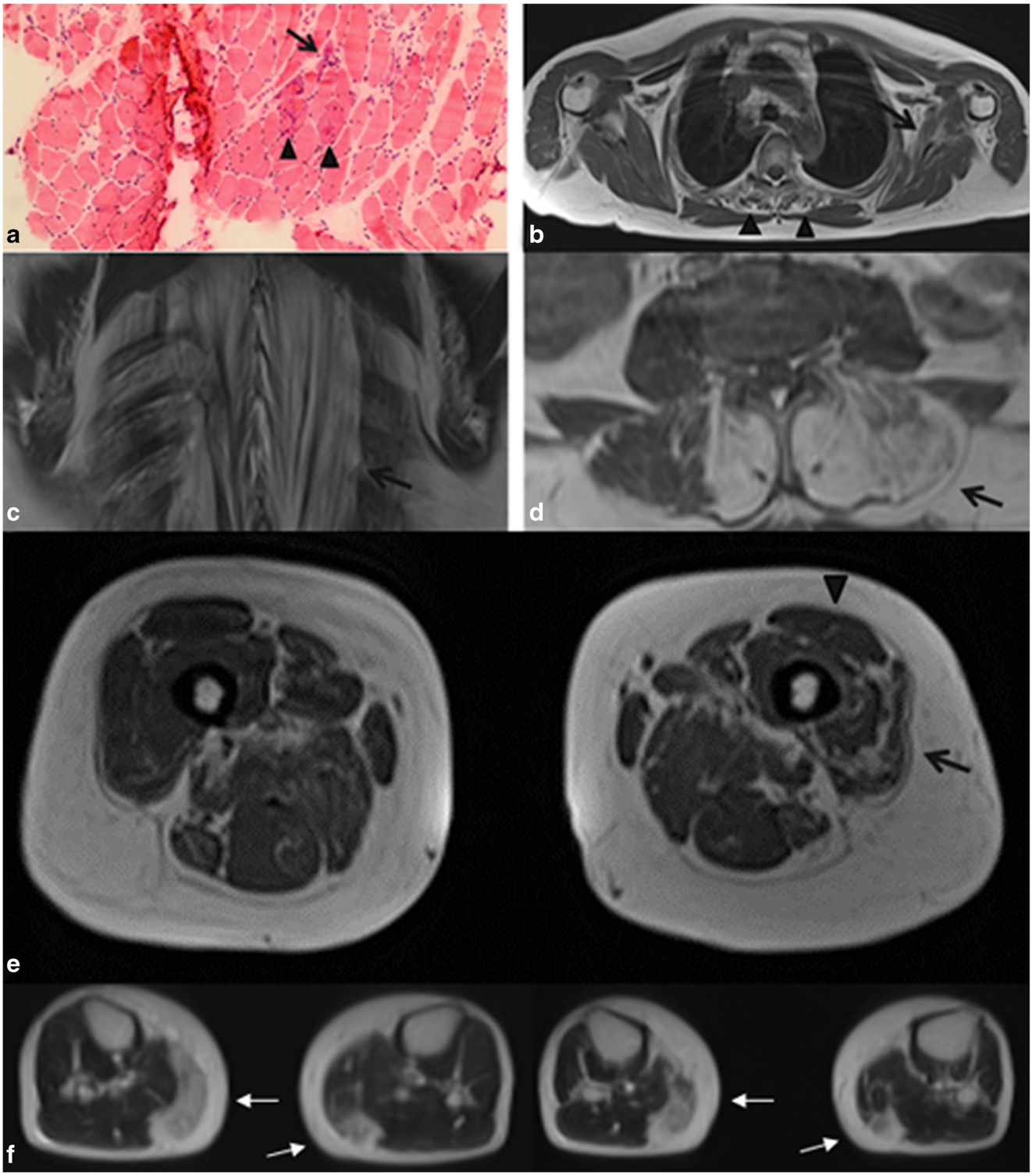

Fig. 3 A 72-year-old female with sporadic inclusion body myopathy (s-IBM). **a** A muscle (H&E in frozen tissue) biopsy shows marked variability in fiber size with endomysial fibrosis. Some mononuclear inflammatory cells are present in the endomysium (*arrow*). Some typical rimmed vacuoles can be seen in the central muscle fibers (*arrowheads*). **b** Axial T1-weighted WBMRI of the shoulder girdle shows mild atrophy of the paraspinal muscles (*arrowheads*) and the left subscapularis muscle (*arrow*). **c**, **d** Coronal (**c**) and axial (**d**) T1-weighted WBMRI of the thoracic and lumbar area, respectively, showing non-symmetrical atrophy of the paraspinal muscles (*arrows*). **e** Axial T1-weighted WBMRI of the thighs showing asymmetric involvement of the left vastus lateralis (*arrow*) with relative sparing of the rectus femoris (*arrowhead*) and posterior muscles. **f** Axial T1-weighted WBMRI of calves shows fatty involvement of medial gastrocnemius (*arrows*). These findings are considered a typical pattern of this entity. IBM mainly involves "ventrally located muscles" rather than "dorsally located muscles" of the extremities. It may also present an asymmetrical pattern

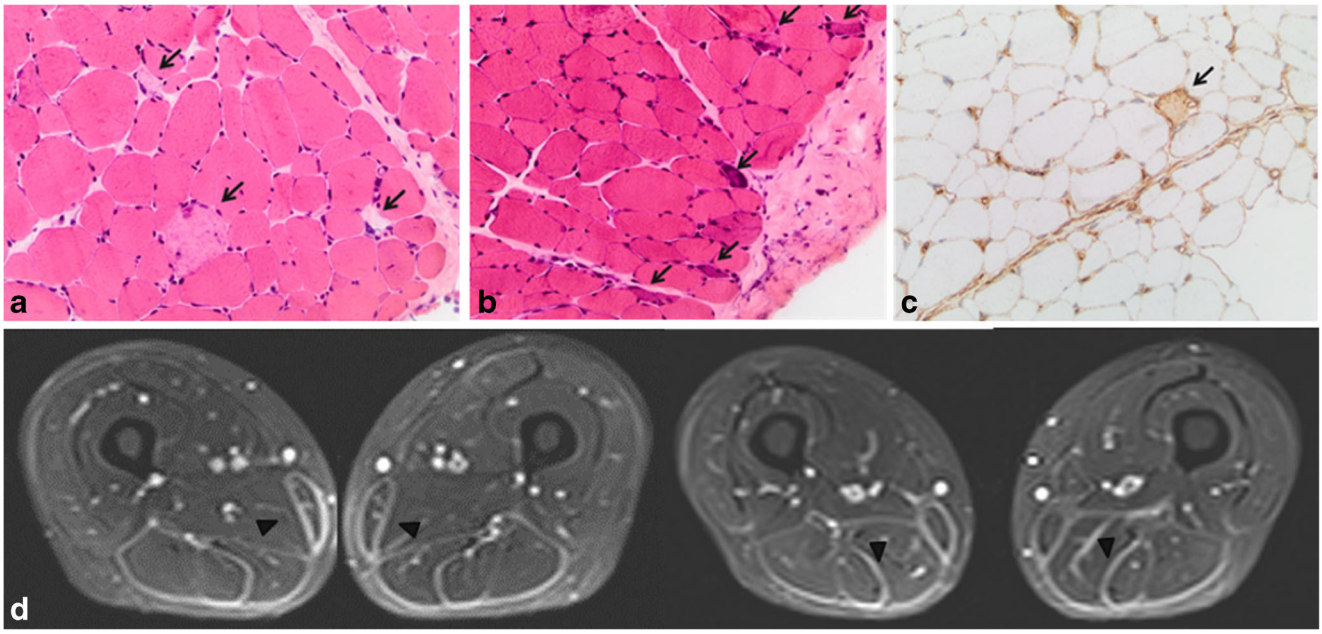

Fig. 4 A 38-year-old woman with necrotizing autoimmune myopathy (NAM). **a**, **b** Muscle biopsy slides (H&E in frozen tissue) showing variability in muscle fiber size with some necrotic muscle cells (**a**; *arrows*) and some regenerating basophilic muscle cells (**b**; *arrows*). Note the absence of significant inflammation. **c** Universal MHC class I sarcolemma positivity (H&E in frozen tissue). A single necrotic cell is seen (*arrow*). Positive endothelial cells can also be observed. **d** Axial STIR-weighted WBMRI of the thighs demonstrates an marked symmetric fascial edema of the hamstring muscles (*arrowheads*). Other inflammatory myopathies and other entities such as Churg–Strauss, myositis, neoplasm, myonecrosis, necrotizing fasciitis, and compartment syndrome may show fascial thickening

IIM [51]. Schanz et al. described bilateral symmetrical generalized myositis in 14/18 (78%) patients with overlap myositis and systemic sclerosis (Fig. 7). The presence of edema is explained by an increased amount of fluid and inflammatory infiltration. In up to one-third of the cases of PM, an underlying systemic autoimmune disease may be identified [52, 53]. A scleroderma-like disorder, eosinophilic fasciitis (EF), is an uncommon

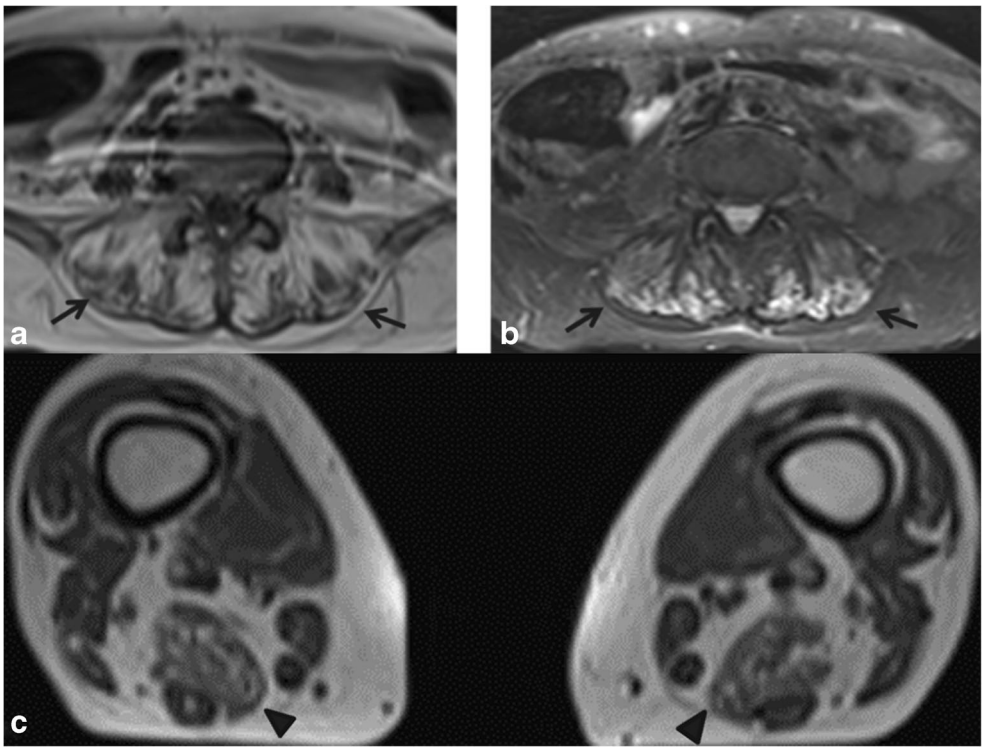

Fig. 5 A 75-year-old woman with necrotizing autoimmune myopathy (NAM). **a**, **b** Axial T1-weighted (**a**) and STIR-weighted WBMRI (**b**) of the lumbar spine. Symmetrical atrophy and edema of paraspinal muscles respectively (*arrows*). **c** Axial-T1 weighted WBMRI of the thighs shows symmetric mild atrophy of the hamstring muscles (*arrowheads*)

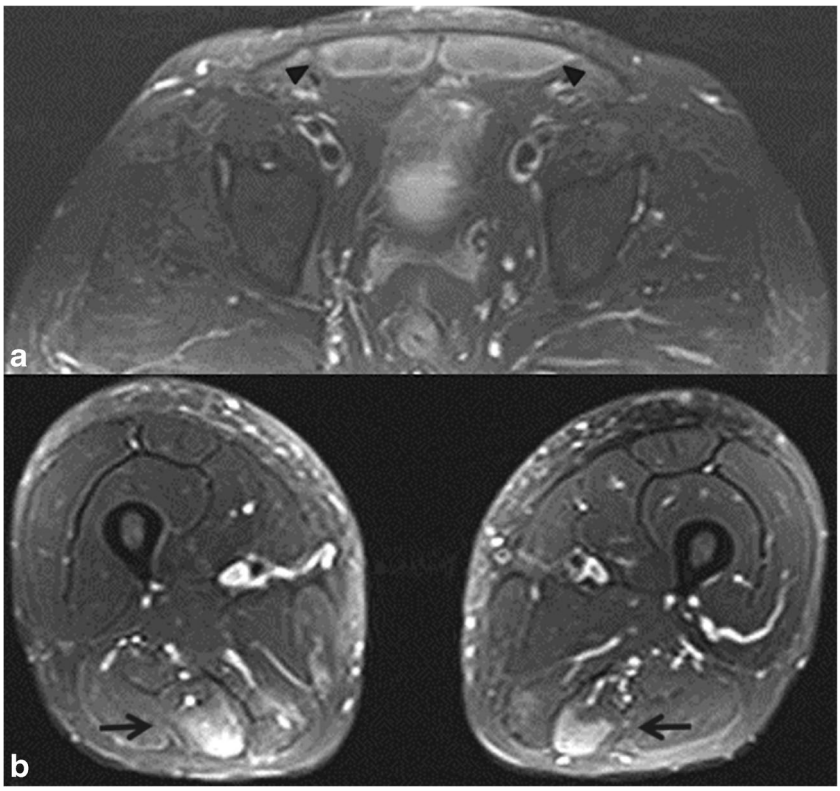

Fig. 6 A 68-year-old female with necrotizing autoimmune myopathy (NAM). **a** Axial STIR-weighted WBMRI of the pelvic girdle demonstrates symmetric edema of the rectus abdominis muscles (*arrowheads*) and **b** the semimembranosus muscles (*arrows*)

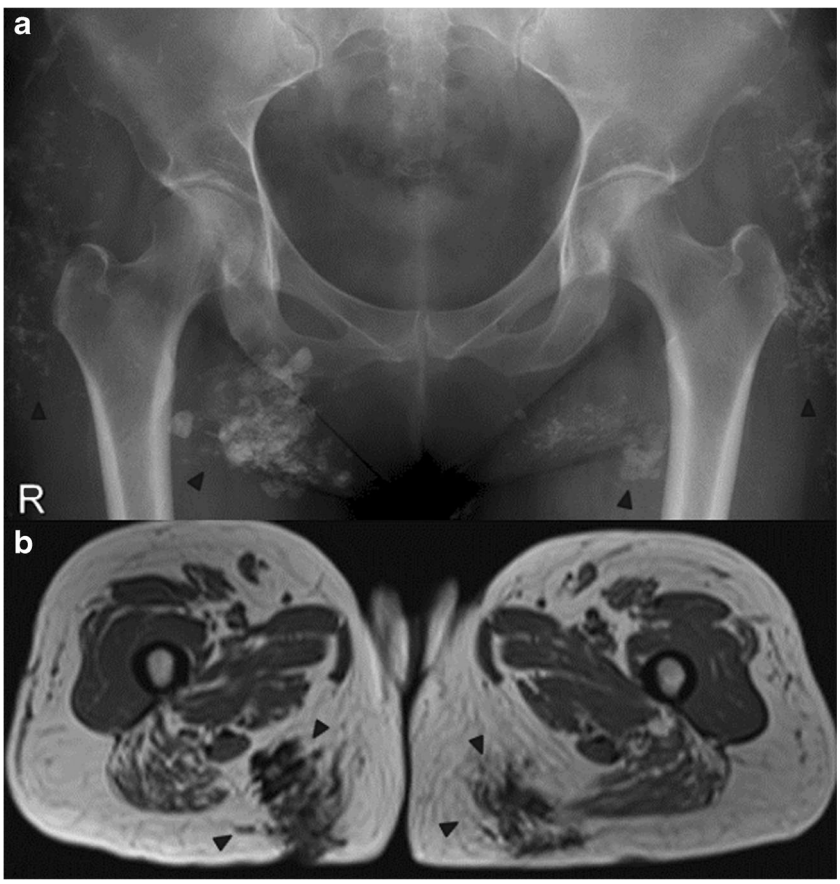

Fig. 7 A 49-year-old female with dermatomyositis and systemic sclerosis; overlap syndrome. **a** Pelvic radiograph and **b** axial T1-weighted WBMRI shows coarse subcutaneous calcifications (*arrowheads*)

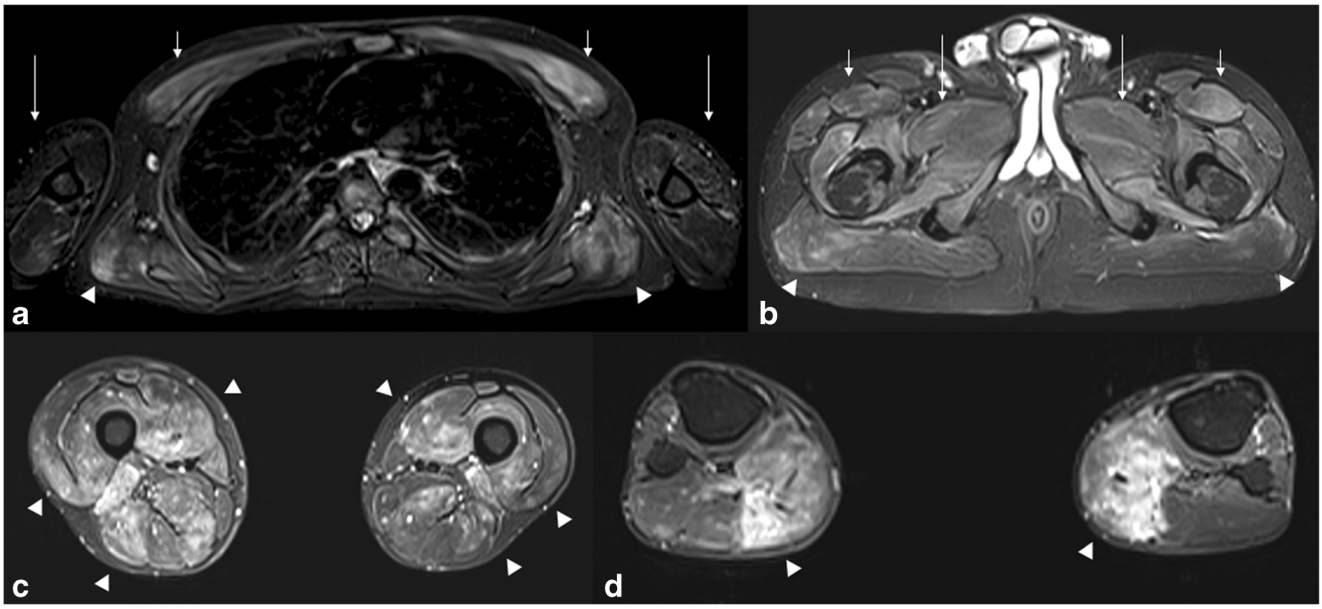

Fig. 8 A 31-year-old man with eosinophilic fasciitis (EF) with subjacent myositis. Axial STIR-weighted WBMRI. **a** Symmetric, diffuse edema of the latissimus dorsi (*arrowheads*), pectoralis major (*short arrows*) and arm muscles (*long arrows*). **b** Pelvic girdle. Bilateral edema of the gluteus maximus (*arrowheads*), proximal thigh muscles (*short arrows*), adductor fascia and muscles (*long arrows*). **c** Severe, diffuse bilateral edema of the three fascial compartments that divide and contain the thigh muscles (*arrowheads*). **d** Bilateral symmetric edema of the medial gastrocnemius (*arrowheads*). EF is a rare scleroderma-like disorder that can be associated with myositis. In the acute phase of the disease, MRI shows a markedly increased signal intensity within the fascia and muscles on fluid-sensitive STIR-weighted sequences

Table 2 Idiopathic inflammatory myopathies (IIMs). Anatomical distribution

	Head/neck Upper limb girdle	Thorax Abdomen	Lower limb girdle	Thighs	Legs	Miscellaneous
Dermatomyositis	++ Bilateral symmetrical muscle and fascial edema	+	++ Bilateral symmetrical muscle, **subcutaneous** and fascial edema	+++ Bilateral symmetrical muscle (quadriceps) **subcutaneous** and fascial edema	+	Heliotrope Gottron's sign Subcutaneous calcifications Neoplasms
Polymyositis	+++ Bilateral symmetrical muscle and fascial edema	+	++ Bilateral symmetrical muscle and fascial edema	+++ Bilateral symmetrical muscle (adductors)[a] and fascial edema	+	Dysphagia Neoplasms
Sporadic inclusion-body myositis (s-IBM)	++ Wrist and deep finger flexors ++ Axial muscles **Camptocormia** **Head drop**	++ Atrophy of the axial muscles; **Camptocormia** **Head drop**	Adductor and abductor muscles are relatively spared	+++ Quadriceps muscle (with relative sparing of the rectus femoris), distal sartorius	+++ Atrophy of the medial gastrocnemius, ankle dorsiflexors	Dysphagia "ventrally located > dorsally located muscles"[a] 10–44% are asymmetrical
Necrotizing autoimmune myopathy (NAM)		++ Paraspinal muscles[b] ++ Rectus abdominis muscles[b]		+++ Atrophy hamstrings and adductor magnus +++ Edema vastus lateralis; relative sparing of the vastus intermedius[a]		Statins-related
Overlap syndrome	++ Bilateral symmetrical edema of proximal muscles.		**Subcutaneous calcifications**	++ Bilateral symmetrical edema of proximal muscles		**Systemic sclerosis** Lupus Eosinophilic fasciitis

Boldface values indicate the important finding

[a] Not present in our study

[b] Rare finding identified in our study

connective tissue disorder that can present with muscle symptoms mimicking other neuromuscular diseases [54]. EF is characterized by an abrupt onset of edema, followed by progressive induration of primarily the distal extremities with symmetrical scleroderma-like indurations of the skin and pain. Patients may show inflammatory arthritis, joint contractures, decreased mobility, and nerve entrapment. Almost half of patients with EF have coexisting morphea plaques. Classic laboratory studies report peripheral eosinophilia, hypergammaglobulinemia, and elevated inflammatory markers. EF is included within the spectrum of scleroderma-like disorders and may be difficult to differentiate from other sclerosing skin disorders [55]. Although fascial biopsy has classically been considered the gold standard for diagnosing EF, radiologic imaging techniques, especially MRI, have been increasingly used for both the diagnosis and monitoring of treatment response [56]. MRI of the thighs has demonstrated superficial and deep fascial thickening with T2 hyperintensity. Some cases may show lymphocytic infiltration and degeneration of the underlying muscle, leading to a diagnosis of EF associated with myositis (Fig. 8) [54, 57]. Other entities beyond inflammatory myopathies such as Churg–Strauss, myositis, neoplasm, myonecrosis, necrotizing fasciitis, and compartment syndrome may show fascial thickening [58] (Table 2).

Dystrophic myopathies

Dystrophinopathies (Duchenne and Becker muscular dystrophies)

Muscular dystrophies are a heterogeneous group of slowly progressive and disabling myopathies which, in most cases, present with proximal pelvic girdle and shoulder girdle weakness. The most common and severe muscular dystrophy is called Duchenne muscular dystrophy, which is an X-chromosomal recessive disorder presenting during childhood

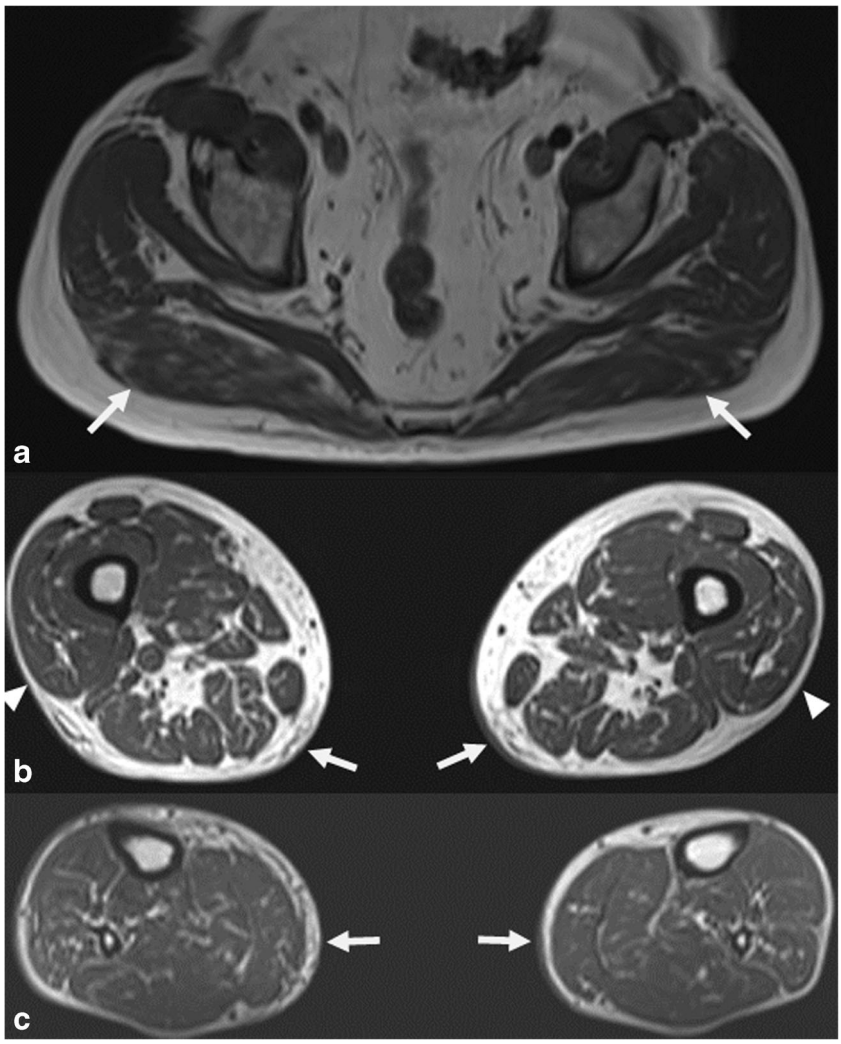

Fig. 9 A 69-year-old male showing MRI signs suggestive of Becker muscular dystrophy. This case was finally diagnosed as a distal muscular dystrophy. Axial T1-weighted WBMRI of the pelvic girdle (**a**) showing symmetrical mild atrophy of gluteal muscles (*arrows*), thighs (**b**); mild atrophy of the semimembranosus (*arrows*) and moderate atrophy of the vastus externus (*arrowheads*), and legs (**c**); the soleus and gastrocnemius muscles are spared (*arrows*)

and characterized by the absence of dystrophin [59]. Beginning in the thighs, muscle fibers become necrotic, and over time, are replaced by fat and connective tissue. As opposed to the complete absence of dystrophin observed in Duchenne, Becker muscular dystrophy is characterized by the presence of a partially functional dystrophin protein. The clinical symptoms of these dystrophinopathies range from minimal to severe [60]. MRI can assess the extension of muscle atrophy and fatty replacement, including subclinical stages [61]. Qualitative scores have been developed to evaluate these diseases. The four-point Mercuri score [62] ranges from "0" (normal appearance) to "4" (end-stage disease involving complete replacement of muscle by fat and connective tissue, detected by a lower density in CT, or T1-weighted hyperintense signal in MRI). STIR MRI sequence allows early detection of muscle edema, which is helpful in younger children, in whom fatty atrophy is not yet a prominent feature [63]. The MRI pattern of muscle involvement in Becker muscular dystrophy (Fig. 9) can grossly affect the same anatomic areas as Duchenne dystrophy, albeit with milder intensity [60, 64,

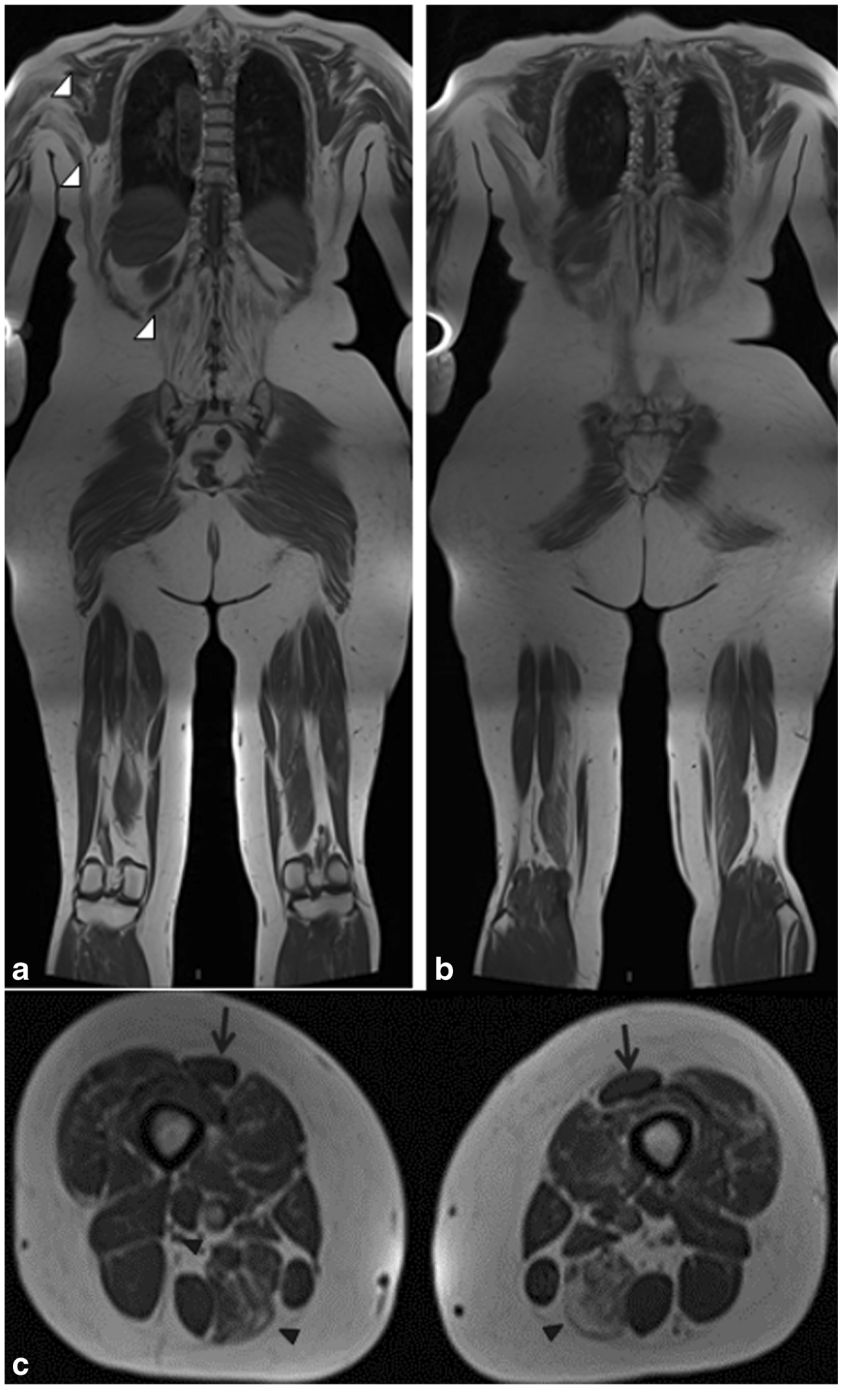

Fig. 10 A 56-year-old female with facioscapulohumeral muscular dystrophy (FSMD) type 2 SSLP 161166. **a**, **b** Coronal T1-weighted WBMRI depicts symmetric atrophy of the shoulder girdle, arms, thoracic wall, and paraspinal muscles (*arrowheads*). **c** Axial T1-weighted WBMRI of the thighs shows moderate atrophy of quadriceps (with sparing of the rectus femoris; *arrows*) and semimembranosus muscles (mainly left; *arrowheads*). This symmetric and extended pattern is unusual in patients with FSMD

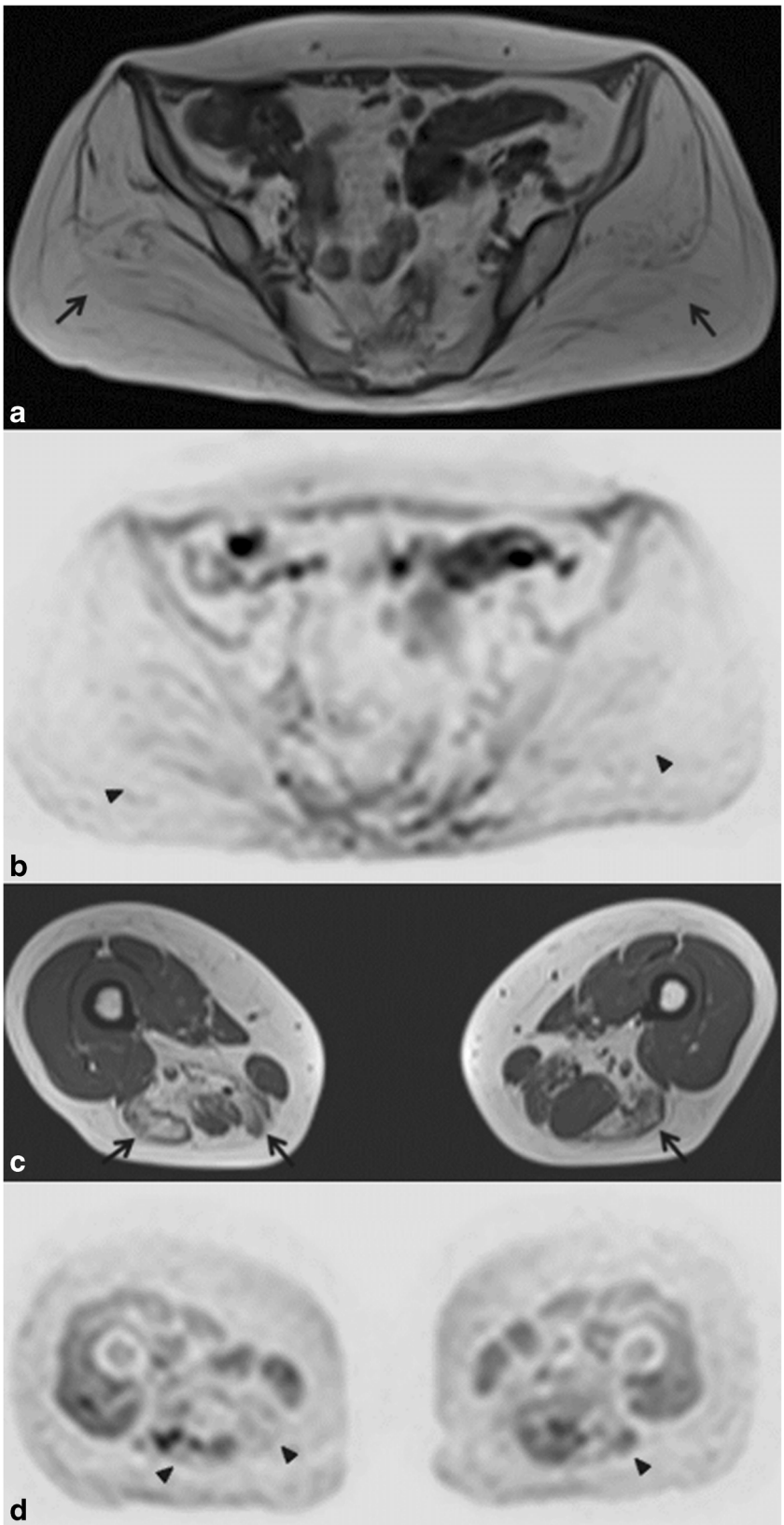

Fig. 11 A 59-year-old female with limb girdle muscular dystrophy (LGMD). **a** Comparative axial T1-weighted and **b** inverted gray-scale with a b-value of 800 s/mm^2 diffusion-weighted WBMRI of the pelvic girdle showing extreme bilateral atrophy of the gluteal muscles (*arrows*) and decreased signal ("T2 blackout effect") of the same muscles (*arrowheads*). **c** Comparative axial T1-weighted and **d** inverted gray-scale with a b-value of 800 s/mm^2 diffusion-weighted WBMRI of the thighs shows mainly atrophy of the right biceps femoris and semimembranosus muscles and of the left biceps femoris muscle (*arrows*) with decreased signal ("T2 blackout effect") of the same muscles (*arrowheads*). The sartorius and gracilis muscles are spared

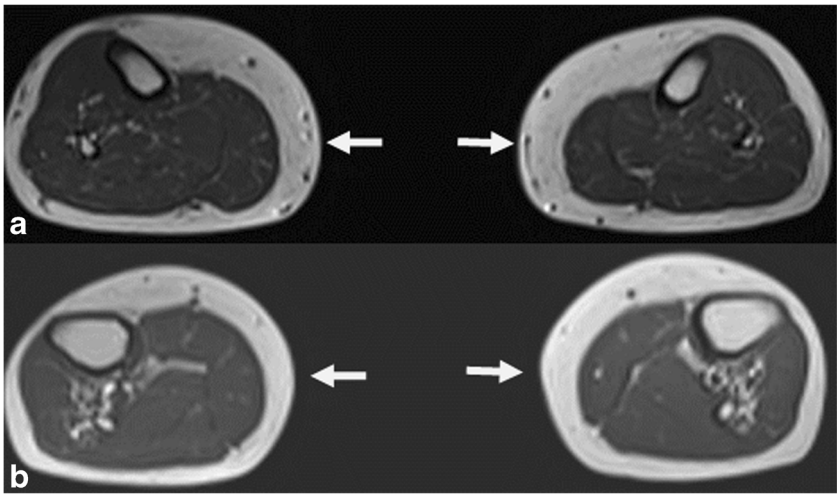

Fig. 12 **a** A 56-year-old female with facioscapulohumeral muscular dystrophy (FSMD). **b** A 59-year-old female with limb girdle muscular dystrophy (LGMD). Axial T1-weighted WBMRI of the legs. Neither patient (the same patients as in Figs. 10 and 11, respectively) showed the previously reported sign of fatty replacement of the gastrocnemius. In both cases, the morphology of the gastrocnemius was normal (*arrows*)

65] and with the upper extremities being less commonly affected [66]. Patients with Duchenne muscular dystrophy present a distinctive pattern according to the severity of fat replacement; in severe fat replacement the gluteus medius and minimus, the biceps femoris and adductor magnus muscles are affected while in moderate-to-severe fat replacement the gluteus maximus and quadriceps are involved; lastly, in cases with the absence of or low fat replacement, the gracilis, sartorius, long adductor, and semimembranous are completely spared [67].

Myotonic dystrophy (MD) and facioscapulohumeral muscular dystrophy (FSMD)

Among the different types of muscular dystrophy, MD type I dystrophy (Steinert's disease) and FSMD are the second and third most common worldwide, respectively. The so-called "Beevor's sign" consists of an upward movement of the umbilicus towards the head on flexing the neck when in a supine position or sitting up due to a spinal injury leading the rectus abdominis muscle to remain intact but the lower part weak, and may be present in FSMD, Pompe's disease and s-IBM [68]. A new "extended-Beevor's sign" has recently been described in a patient with s-IBM. This patient presented a deviation of the umbilicus to the right while when standing due to asymmetric involvement of the right paraspinal muscle with indemnity of the right abdominal oblique muscle [69]. MD and FSMD are characterized by facial and distal muscle weakness and wasting of the forearm, the anterior part of the thighs, with a relatively spared rectus femoris (Fig. 10), and presents a

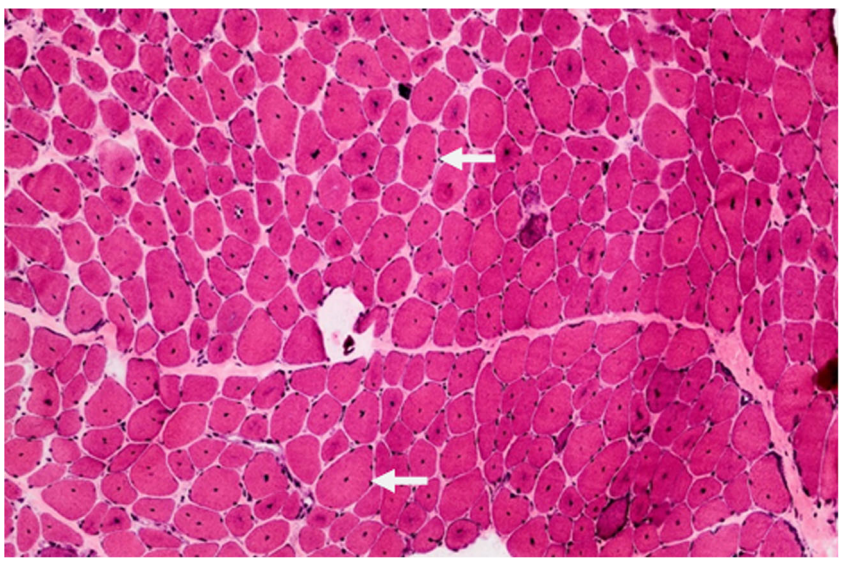

Fig. 13 A 72-year-old female with congenital or non-dystrophic myopathy due to a receptor mutation. The muscle biopsy (hematoxylin and eosin in frozen tissue) shows an abnormal location of the central nucleus in most of the muscle cells ("radial wheel sign"; *arrows*). Centronuclear myopathy derives its name from this central location of the muscle cell nucleus, which is normally located at the periphery of the muscle cell

"semilunar pattern" of involvement [70] and lower leg muscles (especially the medial gastrocnemius and soleus muscles). The tibialis posterior is entirely spared [71]. FSMD patients often show asymmetric leg muscle involvement with distal prominence, mainly of the tibialis anterior and medial gastrocnemius [72].

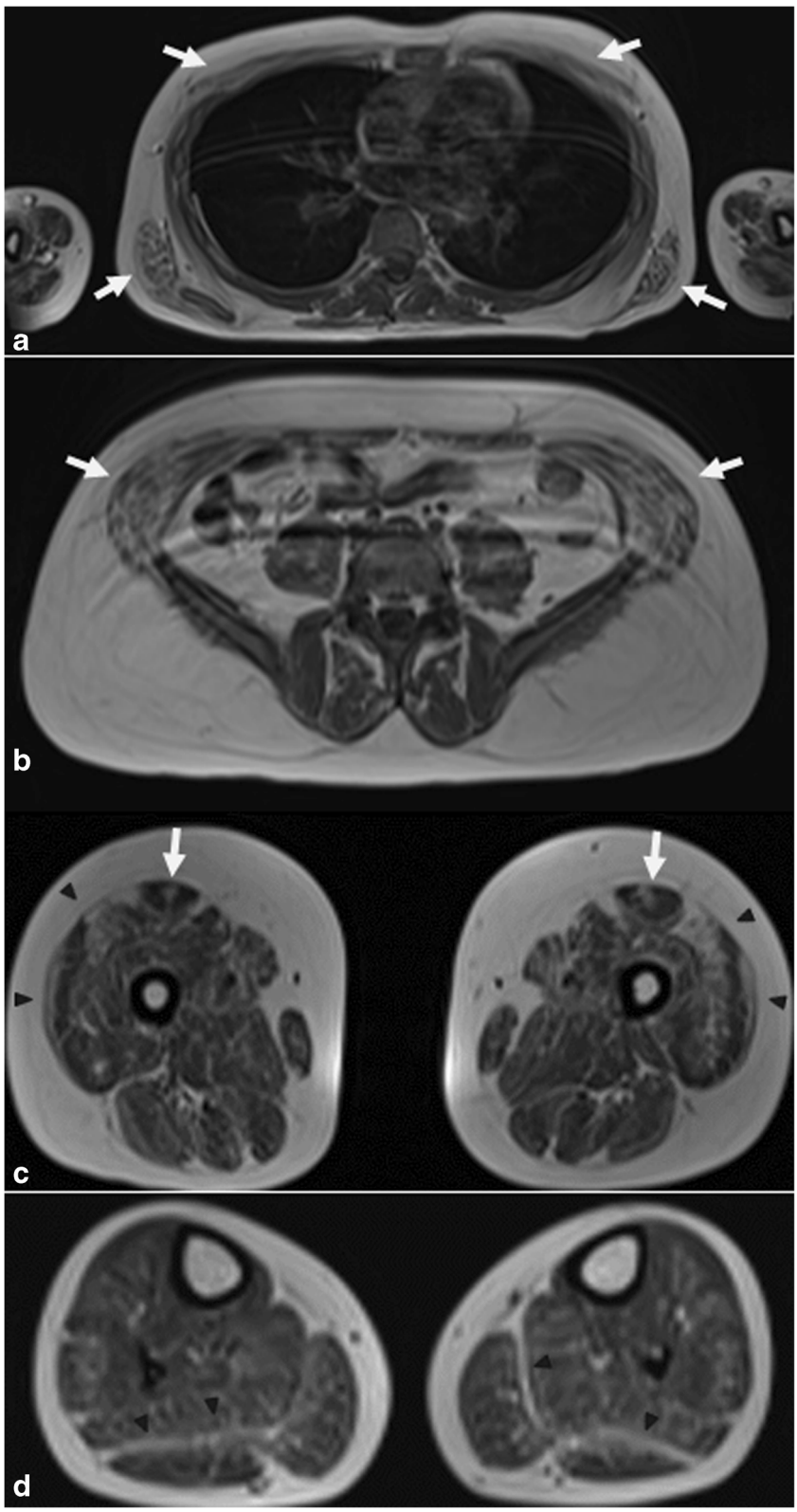

Fig. 14 A 20-year-old male with congenital or non-dystrophic myopathy, known as Bethlem myopathy, associated with collage VI abnormalities. Axial T1-weighted WBMRI. **a** Symmetrical atrophy of the thoracic wall (*arrows*) and **b** abdominal wall muscles (*arrows*). **c** Thighs. "Central shadow" rectus femoris pattern (*arrows*) and "outside-in" rim pattern of vastus externus (*arrowheads*). **d** Legs. Thickening of connective tissues between the soleus and gastrocnemius muscles (*arrowheads*). These MRI signs are strongly suggestive of Bethlem myopathy

Limb girdle muscular dystrophy (LGMD)

LGMD is a heterogeneous group of autosomal dominant and recessive hereditary myopathies. The MRI pattern shows a "Duchenne-like" distribution, with severe fatty replacement in the thigh muscles, mild-to-moderate involvement of the pelvic muscles and sparing of the sartorius and gracilis (Fig. 11) [73, 74]. Other studies have reported some differences in MRI findings between Becker muscular dystrophy (quadriceps affected, gastrocnemius relatively spared) and LGMD (quadriceps spared, gastrocnemius affected) (Fig. 12) [60, 75, 76].

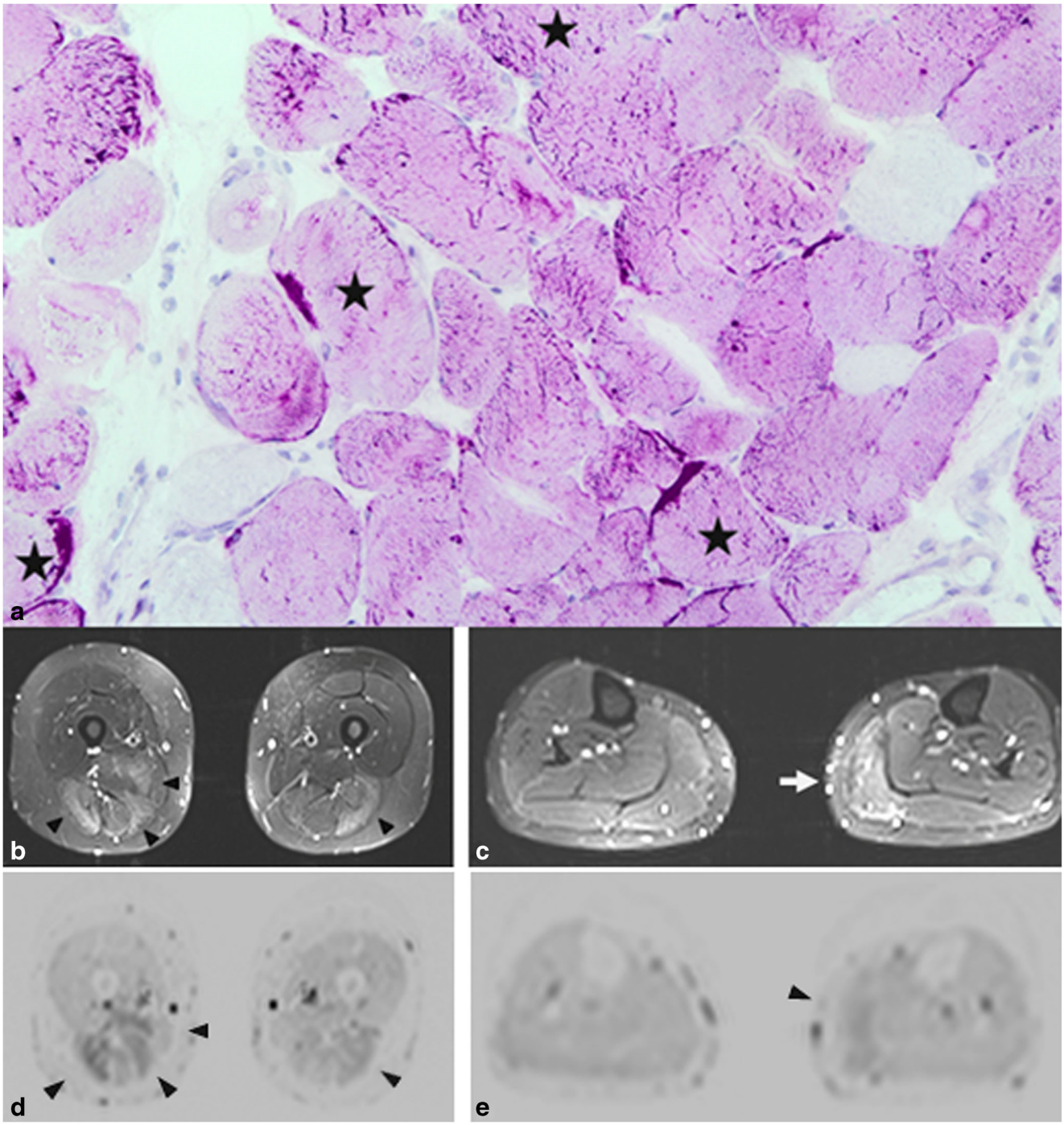

Fig. 15 A 43-year-old female with a glycogen storage disorder. **a** Periodic acid Schiff (PAS) staining in frozen muscle tissue. Subsarcolemic PAS positive material is clearly seen in several muscle fibers (*stars*). **b** Axial STIR-weighted WBMRI of the thighs shows edema of the hamstring muscles (*arrowheads*) and **c** edema of left medial gastrocnemius muscle of the legs (*arrow*). **d**, **e** Inverted gray-scale with a b-value of 800 s/mm^2 diffusion-weighted WBMRI at the same anatomical planes as b and c, respectively, shows increased signal ("T2-shine-through") of the same muscles (*arrowheads*)

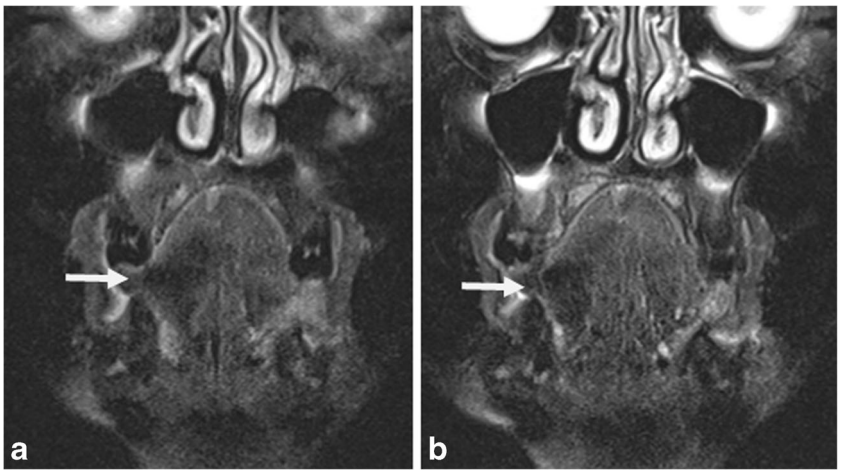

Fig. 16 A 66-year-old female with Pompe disease (type II glycogen storage disorder; metabolic myopathies). **a**, **b** Coronal FST2-weighted with fat-saturation MRI depicts a heterogeneous, low signal in the intrinsic muscles of the tongue and the floor of the mouth, predominantly on the right side (*arrows*). The tongue is a "target area" of severe involvement in Pompe disease and is not visualized in other myopathies

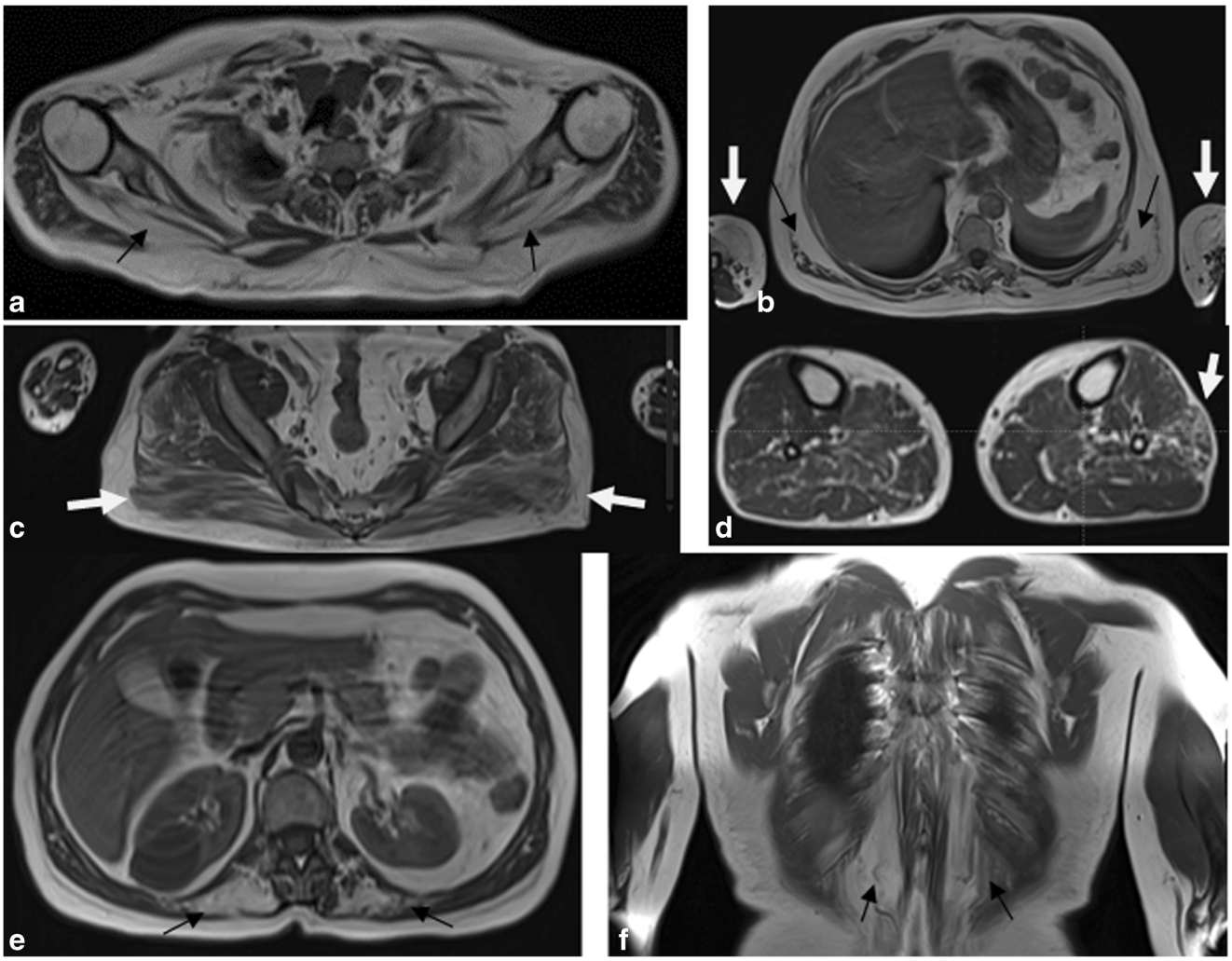

Fig. 17 A 60-year-old female with McArdle disease (type V glycogen storage disorder; metabolic myopathies). T1-weighted WBMRI. **a** Shoulder girdle with symmetrical atrophy of rotator cuff muscles (*arrows*). **b** Thoracic wall with symmetrical atrophy of the biceps and thoracic muscles (*arrows*). **c** Pelvic girdle with atrophy of the gluteal (medium and major) muscles (*arrows*). **d** Legs with asymmetrical, bulky atrophy of the left peroneus muscles (*arrow*). **e**, **f** Symmetric atrophy of the paraspinal muscles (*arrows*). This MRI sign has been previously reported as being "rare", but we consider that it could be more frequent than previously published

Congenital or non-dystrophic myopathies (CM)

CM is a heterogeneous group of rare autosomal-dominant or autosomal-recessive myopathies classified according to the predominant histopathologic findings in skeletal muscle. It may be associated with collagen VI abnormalities (Bethlem and Ullrich myopathies) or associated with receptor mutations [9]. "Centronuclear myopathy" is a histopathologic umbrella term that is sometimes used in association with some of these mutational diseases. In centronuclear myopathy, the cell nucleus, which is normally located at the periphery of the muscle cell, is in a central position (Fig. 13). Bethlem myopathy and the more severe Ullrich congenital muscular myopathy are characterized by contractures that typically affect the fingers and elbows, and these patients also present spinal rigidity. MRI may show a characteristic "outside-in" pattern, with pathologic outer rim of muscle with relative sparing of the muscle belly [77, 78]. Another interesting finding is thickening of the connective tissues between muscles, such as the rectus femoris ("central-shadow") soleus and gastrocnemius (Fig. 14) [78]. In CM associated with receptor mutations, the patients present muscle weakness at birth or the onset of permanent symptoms during childhood [79], usually with very slowly progressive muscle weakness [80]. The cranio-facial, pelvic girdle, and limb muscles may show fatty replacement, with different previously described MRI patterns showing muscle fatty replacement in different subgroups [81]. For instance, the quadriceps and gastrocnemius are relatively spared in ACTA 1-related myopathy. In contrast, in patients with RYR1 mutations, the quadriceps muscle is frequently affected with relative sparing of the rectus femoris muscle [82, 83].

Metabolic myopathies, glycogen storage disorders (GSD)

Glycogen storage disorders are the result of defects in the processing of glycogen synthesis within the muscles, liver, and other tissues. Up to 11 different diseases have been

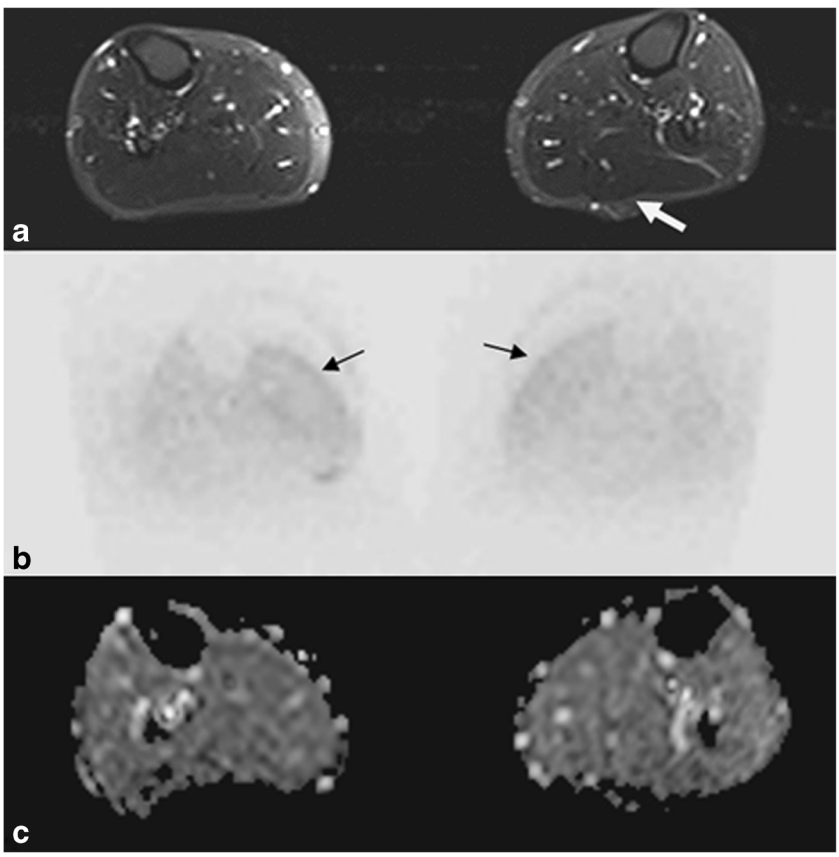

Fig. 18 A 74-year-old male with muscle channelopathy. **a** Axial STIR-weighted WBMRI of the legs depicts a subtle bulk of the left lateral gastrocnemius (*arrow*). No other previously reported MRI findings such as degeneration of the gastrocnemius muscles or a semilunar pattern of the quadriceps muscle sparing the rectus femoris were found in this patient. In most cases, channelopathies do not generally show pathological MRI findings such as fatty replacement or muscle edema. **b** However, an axial inverted gray-scale with a b-value of 800 s/mm^2 DWI WBMRI of the legs showed an increased signal with no significant concordant signal abnormality on the ADC map (**c**), consistent with diffusion restriction and T2-shine-through of the medial gastrocnemius muscles (*arrows*). Although DWI with ADC mapping is being explored for evaluation of ADC maps, its current potential uses include qualitative detection of signal abnormalities on DWI that are occult on STIR, targeting for biopsy and treatment response

reported, some of which can potentially cause muscle damage. Several examples of GSD with muscle involvement are: type II (Pompe disease), due to acid maltase deficiency, an autosomal recessive disorder caused by a deficiency of alpha-glucosidase activity; type III (Cori's or Forbes disease), due to a deficiency of the glycogen disbranching enzyme, and type V (McArdle disease), due to muscle glycogen myophosphorylase deficiency. These subgroups can target the muscular system (Fig. 15). Symptom severity and onset depend on the amount of enzymatic deficiency. Timely diagnosis is important to implement the early treatment with enzyme replacement therapy [84]. MRI in patients with Pompe disease has shown relative sparing of the rectus femoris, sartorius, gracilis, and superficial vastus laterals, whereas the tongue (Fig. 16), adductor magnus, and anterior arm muscles have shown severe involvement [85–87]. McArdle disease is extremely rare in patients under 40 years old, but when present, wasting usually affects the shoulder girdle [88]. Axial involvement of paraspinal muscles has been exceptionally reported [89], but we have found this finding in two patients (Fig. 17).

Muscle channelopathies

Electrical hyperexcitability or inexcitability due to changes in ionic conductivities (defective ion channels) of the muscle fiber membrane is the physio-pathological origin of muscle myotonia and paralysis, respectively. Non-dystrophic myotonias and periodic paralysis are the main early episodic symptoms observed in

Table 3 Non-idiopathic inflammatory myopathies. Anatomical distribution

	Head/neck upper limb girdle	Thorax abdomen	Lower limb girdle	Thighs	Legs	Miscellaneous
Dystrophinopathies (Duchenne and Becker muscular dystrophy)	++ Bilateral symmetrical muscle atrophy		++ Bilateral symmetrical muscle atrophy	++ Bilateral symmetrical muscle atrophy	Gastrocnemius relatively spared	X-chromosome recessive disorders **Severity Duchenne > Becker**
Myotonic dystrophy (MD) and facioscapulohumeral muscular dystrophy (FSMD)	Facial and distal muscle weakness and wasting of the forearm	++ Symmetric atrophy of thoracic wall and paraspinal muscles[b]		++ Anterior part of the thighs, with a relatively spared rectus femoris **(semilunar pattern)** +semimembranosus[b]	++ Medial heads of gastrocnemius, soleus[a] The tibialis posterior is entirely spared	
Limb girdle muscular dystrophy (LGMD)			+/++ Atrophy	+++ Atrophy Sparing of the sartorius and gracilis	+++Gastrocnemius[a]	
Congenital or non-dystrophic myopathies (Ullrich and Bethlem diseases)		++ Symmetric atrophy of thoracic and abdominal wall muscles[b]		**"Outside-in" pattern** **"Central shadow"** of the rectus femoris	**"Central-shadow"** of the soleus and gastrocnemius Septal thickening	"Centronuclear myopathies" **Severity Ullrich > Bethlem**
Type II glycogen storage disorder (Pompe)	++ **Tongue** +++ Anterior arm muscles			+++ Adductor magnus. Sparing of the rectus femoris, sartorius, gracilis and vastus lateralis		
Type V clycogen storage disorder (McArdle)	+++ Shoulder girdle	0/+ Paraspinal muscles[b]				
Channelopathies				Muscle bulk hypertrophy of thighs[a] Perifemoral semilunar pattern of quadriceps muscle sparing the rectus femoris[a]	Muscle bulk hypertrophy of calves Early degeneration of gastrocnemius muscles[a] **DWI (b800) increased signal of gastrocnemius[b]**	Disturbances in the serum K+ level Periodic paralysis **Do not generally show pathologic MRI findings**

Boldface values indicate the important finding

[a] Not present in our study

[b] Rare finding identified in our study

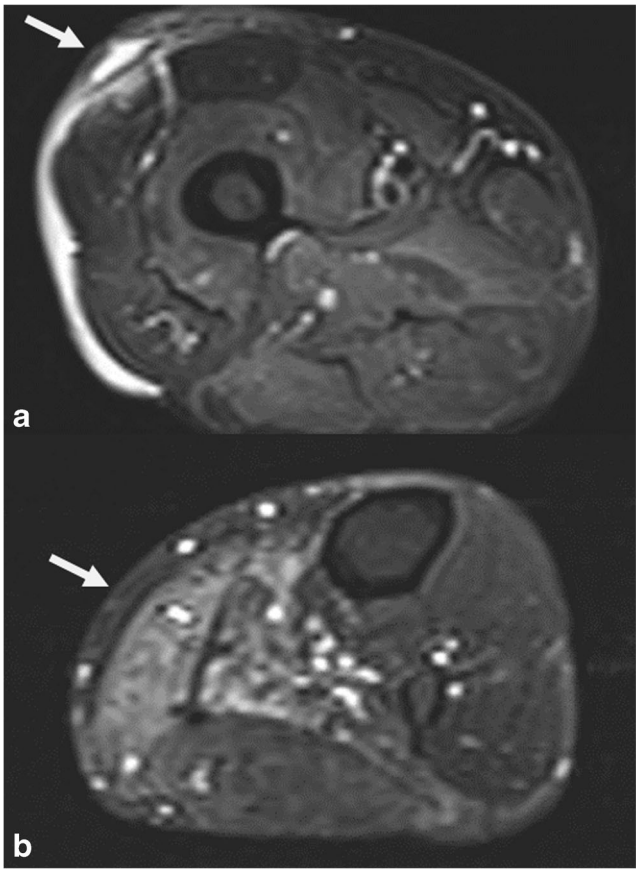

Fig. 19 A 74-year-old male with an unknown myopathy. **a** Axial STIR-weighted WBMRI of the right thigh depicts a mild subcutaneous hematoma after a "blind" biopsy (before WBMRI) of the vastus lateralis muscle (*arrow*). Edema, suggesting the presence of inflammatory activity, is not shown. The biopsy was "negative". **b** In the same axial STIR-weighted WBMRI, edema of the left medial gastrocnemius and soleus muscles (*arrow*) was identified. Based on these WBMRI findings, a second biopsy of the medial gastrocnemius was performed. The biopsy was "positive" for myofibrillar myopathy. WBMRI may increase the yield of muscle biopsy by guiding the biopsy to a site with active inflammation (edema; STIR sequence)

these patients, due to disturbances in serum K+ levels. Progressive focal and general muscle muscular weakness is present in most cases [90]. Slight myopathic changes may be found with increased occurrence of central nuclei and variation of fiber diameter [91]. Channelopathies do not generally show pathological MRI findings such as fatty replacement or muscle edema. However, muscle bulk hypertrophy of thighs and calves (Fig. 18) due to genuine muscle hypertrophy has been reported [71], as well as early degeneration of gastrocnemius muscles and a perifemoral semilunar pattern of quadriceps muscle affection sparing the rectus femoris has been reported [70]. Weber et al. have described promising perspectives with 23Na MRI to elucidate muscular changes in periodic paralyses and other muscular dystrophies [91] (Table 3).

Additional advantages of WBMRI

Imaging-guided muscle biopsy

False-negative results are greatly reduced in MRI-guided biopsies of muscle with edema in IIM patients compared to blind biopsies of clinically involved muscles (rate of non-diagnostic specimen ranges from 10 to 25%) [30]. Another review on the use of STIR sequences reported a sensitivity of 89–100% and a specificity of 80–88% [15]. WBMRI can increase the yield of muscle biopsy by directing the biopsy to a site with active inflammation (edema; STIR sequence) versus areas with fat replacement (T1 sequence), which may have a non-diagnostic histopathology. Therefore, in patients suspected of having myositis, MRI can help to determine the most adequate site for muscle biopsy (Fig. 19) and has shown to be cost-effective in patients with PM [18].

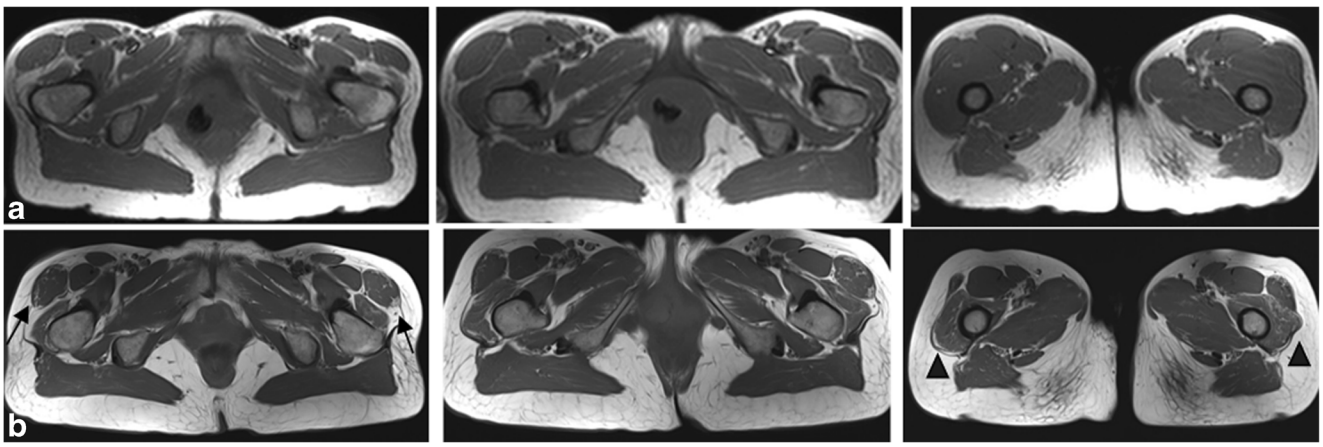

Fig. 20 A 43-year-old female presenting polymyositis with progressive muscle weakness. Comparative axial T1-weighted WBMRI of the pelvic girdle at diagnosis (**a**, *upper images*) and the 3-year follow-up after (**b**, *lower images*) showing new fatty infiltration of tensor fascia lata (*arrows*) and vastus lateralis muscles (*arrowheads*), revealing muscle damage. WBMRI may provide important information and guidance for therapeutic decision-making, differentiating activity of ongoing inflammation (edema) from muscle damage (fatty infiltration)

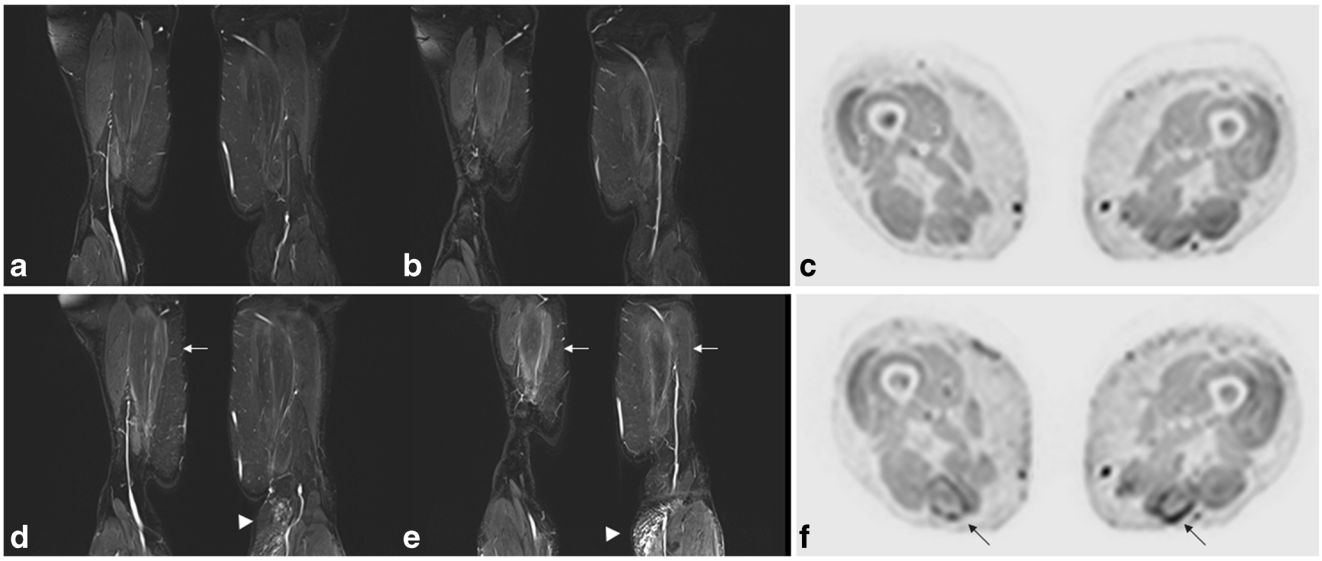

Fig. 21 A 76-year-old female presenting dermatomyositis. Comparative WBMRI of the thighs (same level of slices) at diagnosis (**a**, **b**, **c**) and at 1 year after follow-up (**d**, **e**, **f**). **d**, **e** STIR-weighted coronal pulse sequence shows new edema surrounding semitendinosus and semimembranosus muscles (*arrows*) and subcutaneous tissue (*arrowheads*). **f** DWI of b-value of 800 s/mm^2 WBMRI of the thighs depicts increased signal surrounding semitendinosus muscles (*arrows*). These findings are compatible with ongoing inflammation

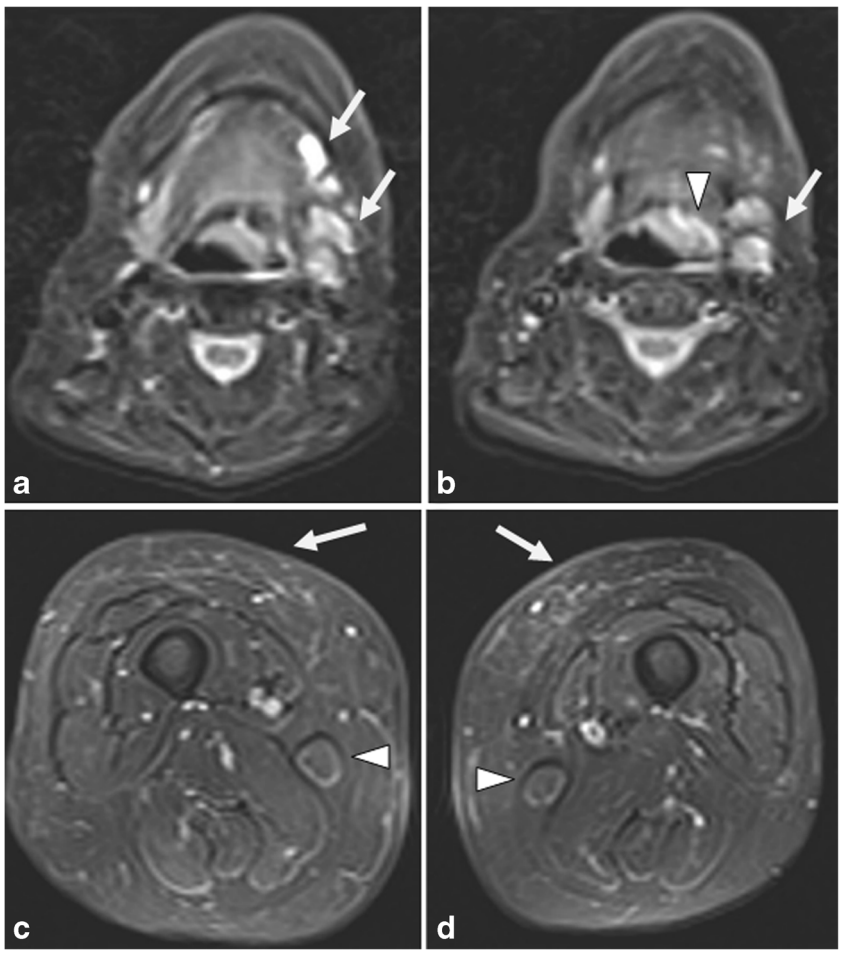

Fig. 22 A 64-year-old female with Sjögren's syndrome and muscle weakness. **a** and **b** Axial STIR-weighted WBMRI of the mandibular area found an incidental left epiglottic mass (*arrowhead*) with regional adenopathies (*arrows*). **c**, **d** Axial STIR-weighted WBMRI of the thighs shows subtle subcutaneous (*arrows*) and fascial edema (*arrowheads*). These findings are frequently observed in dermatomyositis, which can be associated with Sjögren's syndrome. A posterior neck biopsy confirmed a squamous epiglottic cancer. The patient and her referring physician did not keep up with this occult malignancy. WBMRI can stage inflammatory myopathies and detect occult malignancies and/or systemic sclerosis in the same study

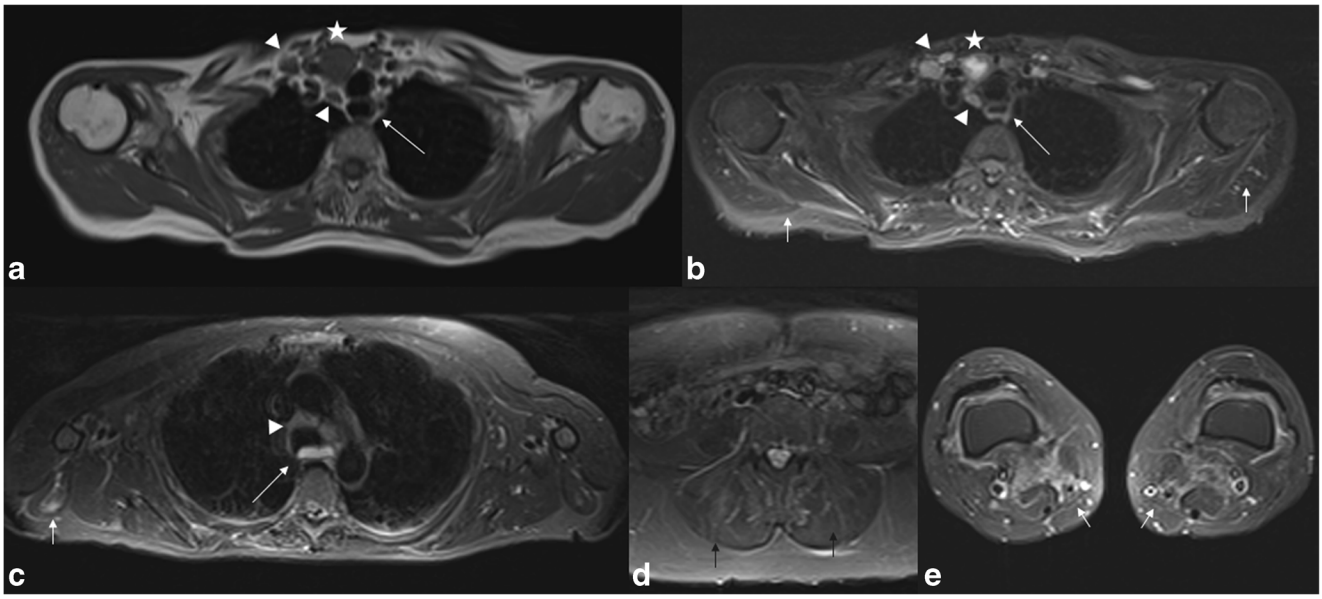

Fig. 23 A 52-year-old female with systemic sclerosis syndrome, breast cancer, and muscle weakness. **a** Axial T1-weighted and **b** axial STIR-weighted WBMRI of the supraclavicular area found an incidental right thyroid mass (*star*) with regional and mediastinal adenopathies (*arrowheads*). The esophagus was dilated (*long arrow*) due to systemic sclerosis. Furthermore, intense fascial edema in the shoulder girdle was found (*short arrows*). **c** Axial STIR-weighted WBMRI caudalad to **b** showed other mediastinal adenopathies (*arrowhead*), a dilated esophagus with fluid (*long arrow*) and edema in the right triceps muscle (*short arrow*). **d**, **e** Axial STIR-weighted WBMRI depicting symmetric edema in the paravertebral muscles (*black arrows*) and popliteal soft tissues (*white arrows*), compatible with an overlap myopathy

Response to therapy, follow-up

It has been reported that clinical improvement seems to be better demonstrated by MRI findings than by muscle biopsy after a short-term follow-up of < 6 months [92]. In patients with persistent muscle weakness, MRI is critical to differentiate active inflammation (STIR/edema) from muscle damage with fatty infiltration (T1/muscle atrophy) (Figs. 20 and 21).

Detection of related and non-related disease

The presence of underlying malignant neoplasms (such as ovarian, breast, and lung cancers), and connective tissue diseases such as systemic sclerosis have shown to be associated with some IIM (DM, PM, and overlap myopathy) [14, 27, 28]. WBMRI can be used to stage these IIMs, as well as to detect occult malignancies or non-related pathologies in the same study (Figs. 22 and 23).

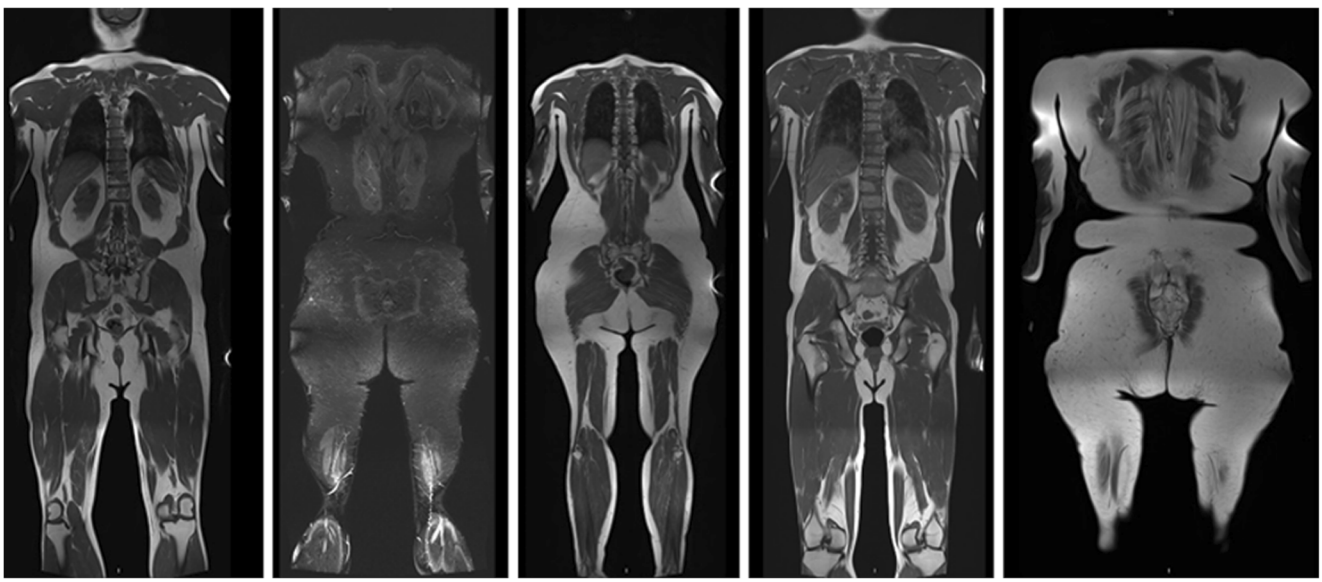

Fig. 24 Coronal T1 and STIR-weighted WBMRI in different cases. Coverage of arms and legs by WBMRI may be incompletely visualized in heavy or tall individuals, respectively. On suspicion of involvement of these areas, the performance of a new dedicated MRI should be considered

The drawbacks of WBMRI

Study duration

The length of a WBMRI study depends on the number of sequences acquired. In our hospital, a complete WBMRI with SET1, STIR, and DWI in axial and coronal planes takes 50–60 min. According to our experience, we strongly recommend beginning with STIR and SET1 axial sequences, which are the most important for evaluating myopathies if the WBMRI procedure has to be discontinued due to patient fatigue.

Patient size

If the patient is too big with respect to the bore width, artifacts (Fig. 24) may hamper the evaluation of the shoulder girdle and/or arms [79]. Involvement of the oculomotor/facial muscles or the calf may be relevant in some myopathies and therefore inclusion of these anatomical areas in the WBMRI is necessary, despite the inherent difficulties in tall patients. In cases showing involvement of these areas (IBM, FSMD, Pompe, among others) a new, dedicated MRI should be considered.

Conclusions

In summary, myopathic signs such as muscle, fascial, and subcutaneous edema (STIR), fatty muscle infiltration (T1) and diffusion imaging values (DWI) can be clearly evaluated in the different muscle compartments using WBMRI, providing a comprehensive estimate of the total burden with a single study. Specific types of myopathy can be identified according to the clinical (Heliotrope, Gottron, Beevor, and extended Beevor), pathological (radial wheel) or MRI signs presented (subcutaneous calcifications or edema, central-shadow rectus femoris, tongue infiltration, etc.). Nevertheless, there are no consensus criteria for the diagnoses of myopathies. Indeed, compared to previous reports, we have found different MRI patterns, including paraspinal muscle involvement (axial myopathy) in two cases of McArdle disease and absence of fatty replacement in the gastrocnemius in LGMD and FSMD.

WBMRI is a diagnostic tool that is useful to determine the most adequate site for muscle biopsy, and to improve the diagnostic accuracy compared to "blind" biopsies. In addition, WBMRI provides important information and guidance for therapeutic decision-making, differentiating activity in terms of ongoing inflammation (edema) from irreversible muscle damage (fatty infiltration). Finally, related and non-related pathological conditions, such as tumors, may be detected in the same imaging study. On the contrary, WBMRI has several limitations in certain anatomical areas such as the arms (artifacts in "large patients"), and the oculomotor/facial muscles or the calf ("tall patients"). On suspicion of involvement of these areas (IBM, FSMD, Pompe, etc.), the performance of a new, dedicated MRI should be kept considered.

Acknowledgements We thank our MRI technicians Santiago Sotes and Irene Millan, and Donna Pringle and Jennifer Brickman for reviewing and improving the manuscript.

Compliance with ethical standards

Conflict of interest The authors declare that they have no conflicts of interest.

Ethical approval All the procedures performed in studies involving human participants were in accordance with the ethical standards of the institutional research committee and with the 1964 Declaration of Helsinki and its later amendments or comparable ethical standards.

Informed consent Informed consent was obtained from all individual participants for whom identifying information is included in this article.

References

1. Findlay AR, Goyal NA, Mozaffar T. An overview of polymyositis and dermatomyositis. Muscle Nerve. 2015;51(5):638–56.
2. Dalakas MC. Inflammatory muscle diseases. N Engl J Med. 2015;373(4):393–4.
3. Pipitone N. Value of MRI in diagnostics and evaluation of myositis. Curr Opin Rheumatol. 2016;28(6):625–30.
4. Curiel RV, Jones R, Brindle K. Magnetic resonance imaging of the idiopathic inflammatory myopathies: structural and clinical aspects. Ann N Y Acad Sci. 2009;1154:101–14.
5. Schmidt GP, Reiser MF, Baur-Melnyk A. Whole-body imaging of the musculoskeletal system: the value of MR imaging. Skelet Radiol. 2007;36(12):1109–19.
6. Filli L, Maurer B, Manoliu A, Andreisek G, Guggenberger R. Whole-body MRI in adult inflammatory myopathies: do we need imaging of the trunk? Eur Radiol. 2015;25(12):3499–07.
7. Del Grande F, Carrino JA, Del Grande M, Mammen AL, Christopher Stine L. Magnetic resonance imaging of inflammatory myopathies. Top Magn Reson Imaging. 2011;22(2):39–43.
8. Yao L, Yip AL, Shrader JA, et al. Magnetic resonance measurement of muscle T2, fat-corrected T2 and fat fraction in the assessment of idiopathic inflammatory myopathies. Rheumatology (Oxford). 2016;55(3):441–9.
9. Zaidman C, Hobson-Webb L. Imaging of skeletal muscle in neuromuscular disease: a clinical perspective. In: Weber MA, editor. Magnetic resonance imaging of the skeletal musculature. Berlin: Springer-Verlag; 2013. p. 3–22.
10. Dobloug C, Garen T, Bitter H, et al. Prevalence and clinical characteristics of adult polymyositis and dermatomyositis; data from a large and unselected Norwegian cohort. Ann Rheum Dis. 2015;74(8):1551–6.
11. Van De Vlekkert J, Maas M, Hoogendijk JE, De Visser M, Van Schaik IN. Combining MRI and muscle biopsy improves diagnostic

accuracy in subacute-onset idiopathic inflammatory myopathy. Muscle Nerve. 2015;51(2):253–8.
12. McCann LJ, Juggins AD, Maillard SM, et al. The juvenile dermatomyositis national registry and repository (UK and Ireland)—clinical characteristics of children recruited within the first 5 years. Rheumatology (Oxford). 2006;45(10):1255–60.
13. Gowdie PJ, Allen RC, Kornberg AJ, Akikusa JD. Clinical features and disease course of patients with juvenile dermatomyositis. Int J Rheum Dis. 2013;16(5):561–7.
14. Maurer B, Walker UA. Role of MRI in diagnosis and management of idiopathic inflammatory myopathies. Curr Rheumatol Rep. 2015;17(11):67.
15. Day J, Patel S, Limaye V. The role of magnetic resonance imaging techniques in evaluation and management of the idiopathic inflammatory myopathies. Semin Arthritis Rheum. 2017;46(5):642–9.
16. Wattjes MP, Kley RA, Fischer D. Neuromuscular imaging in inherited muscle diseases. Eur Radiol. 2010;20(10):2447–60.
17. Malattia C, Damasio MB, Madeo A, et al. Whole-body MRI in the assessment of disease activity in juvenile dermatomyositis. Ann Rheum Dis. 2014;73(6):1083–90.
18. Barsotti S, Zampa V, Talarico R, et al. Thigh magnetic resonance imaging for the evaluation of disease activity in patients with idiopathic inflammatory myopathies followed in a single center. Muscle Nerve. 2016;54(4):666–72.
19. Linklater H, Pipitone N, Rose MR, et al. Classifying idiopathic inflammatory myopathies: comparing the performance of six existing criteria. Clin Exp Rheumatol. 2013;31(5):767–9.
20. Lundberg IE, Miller FW, Tjärnlund A, Bottai M. Diagnosis and classification of idiopathic inflammatory myopathies. J Intern Med. 2016;280(1):39–51.
21. Hoogendijk JE, Amato AA, Lecky BR, Choy EH, Lundberg IE, Rose MR, et al. 119th ENMC international workshop: trial design in adult idiopathic inflammatory myopathies, with the exception of inclusion body myositis, 10-12 October 2003, Naarden, The Netherlands. Neuromuscular disorders : NMD. England; 2004. p. 337–45.
22. Kubínová K, Mann H, Vencovský J. MRI scoring methods used in evaluation of muscle involvement in patients with idiopathic inflammatory myopathies. Curr Opin Rheumatol. 2017;29(6):623–31.
23. Dallaudière B, Lecouvet F, Vande Berg B, et al. Diffusion-weighted MR imaging in musculoskeletal diseases: current concepts. Diagn Interv Imaging. 2015;96(4):327–40.
24. Subhawong TK, Jacobs MA, Fayad LM. Diffusion-weighted MR imaging for characterizing musculoskeletal lesions. Radiographics. 2014;34(5):1163–77.
25. Qi J, Olsen NJ, Price RR, Winston JA, Park JH. Diffusion-weighted imaging of inflammatory myopathies: polymyositis and dermatomyositis. J Magn Reson Imaging. 2008;27(1):212–7.
26. Ai T, Yu K, Gao L, et al. Diffusion tensor imaging in evaluation of thigh muscles in patients with polymyositis and dermatomyositis. Br J Radiol. 2014;87(1043):20140261.
27. Hill CL, Zhang Y, Sigurgeirsson B, et al. Frequency of specific cancer types in dermatomyositis and polymyositis: a population-based study. Lancet. 2001;357(9250):96–100.
28. Chen Y-J, Wu C-Y, Huang Y-L, Wang C-B, Shen J-L, Chang Y-T. Cancer risks of dermatomyositis and polymyositis: a nationwide cohort study in Taiwan. Arthritis Res Ther. 2010;12(2):R70.
29. Garcia J. MRI in inflammatory myopathies. Skelet Radiol. 2000;29(8):425–38.
30. O'Connell MJ, Powell T, Brennan D, Lynch T, McCarthy CJ, Eustace SJ. Whole-body MR imaging in the diagnosis of polymyositis. AJR Am J Roentgenol. 2002;179(4):967–71.
31. Harris-Love MO, Shrader JA, Koziol D, et al. Distribution and severity of weakness among patients with polymyositis, dermatomyositis and juvenile dermatomyositis. Rheumatology (Oxford). 2009;48(2):134–9.
32. Cantwell C, Ryan M, O'Connell M, et al. A comparison of inflammatory myopathies at whole-body turbo STIR MRI. Clin Radiol. 2005;60(2):261–7.
33. Dalakas MC. Inflammatory muscle diseases. N Engl J Med. 2015;372(18):1734–47.
34. Dion E, Cherin P, Payan C, et al. Magnetic resonance imaging criteria for distinguishing between inclusion body myositis and polymyositis. J Rheumatol. 2002;29(9):1897–06.
35. Zheng Y, Liu L, Wang L, et al. Magnetic resonance imaging changes of thigh muscles in myopathy with antibodies to signal recognition particle. Rheumatology (Oxford). 2015;54(6):1017–24.
36. Luo Y-B, Mastaglia FL. Dermatomyositis, polymyositis and immune-mediated necrotising myopathies. Biochim Biophys Acta. 2015;1852(4):622–32.
37. Badrising UA, Maat-Schieman M, van Duinen SG, et al. Epidemiology of inclusion body myositis in the Netherlands: a nationwide study. Neurology. 2000;55(9):1385–7.
38. Wilson FC, Ytterberg SR, St Sauver JL, Reed AM. Epidemiology of sporadic inclusion body myositis and polymyositis in Olmsted County, Minnesota. J Rheumatol. 2008;35(3):445–7.
39. Askanas V, Engel WK, Nogalska A. Sporadic inclusion-body myositis: a degenerative muscle disease associated with aging, impaired muscle protein homeostasis and abnormal mitophagy. Biochim Biophys Acta. 2015;1852(4):633–43.
40. Needham M, Mastaglia FL. Inclusion body myositis: current pathogenetic concepts and diagnostic and therapeutic approaches. Lancet Neurol. 2007;6(7):620–31.
41. Cox FM, Titulaer MJ, Sont JK, Wintzen AR, Verschuuren JJGM, Badrising UA. A 12-year follow-up in sporadic inclusion body myositis: an end stage with major disabilities. Brain. 2011;134(Pt 11):3167–75.
42. Kissel JT. Misunderstandings, misperceptions, and mistakes in the management of the inflammatory myopathies. Semin Neurol. 2002;22(1):41–51.
43. Cox FM, Reijnierse M, van Rijswijk CSP, Wintzen AR, Verschuuren JJ, Badrising UA. Magnetic resonance imaging of skeletal muscles in sporadic inclusion body myositis. Rheumatology (Oxford). 2011;50(6):1153–61.
44. Tasca G, Monforte M, De Fino C, Kley RA, Ricci E, Mirabella M. Magnetic resonance imaging pattern recognition in sporadic inclusion-body myositis. Muscle Nerve. 2015;52(6):956–62.
45. van der Meulen MFG, Bronner IM, Hoogendijk JE, Burger H, van Venrooij WJ, Voskuyl AE, et al. Polymyositis: an overdiagnosed entity. Neurology. 2003;61(3):316–21.
46. Stenzel W, Goebel H-H, Aronica E. Review: immune-mediated necrotizing myopathies—a heterogeneous group of diseases with specific myopathological features. Neuropathol Appl Neurobiol. 2012;38(7):632–46.
47. Mammen AL, Chung T, Christopher-Stine L, et al. Autoantibodies against 3-hydroxy-3-methylglutaryl-coenzyme a reductase in patients with statin-associated autoimmune myopathy. Arthritis Rheum. 2011;63(3):713–21.
48. Casciola-Rosen L, Mammen AL. Myositis autoantibodies. Curr Opin Rheumatol. 2012;24(6):602–8.
49. Ernste FC, Reed AM. Idiopathic inflammatory myopathies: current trends in pathogenesis, clinical features, and up-to-date treatment recommendations. Mayo Clin Proc. 2013;88(1):83–105.
50. Pinal-Fernandez I, Casal-Dominguez M, Carrino JA, et al. Thigh muscle MRI in immune-mediated necrotising myopathy: extensive oedema, early muscle damage and role of anti-SRP autoantibodies as a marker of severity. Ann Rheum Dis. 2017;76(4):681–7.
51. Low AHL, Lax M, Johnson SR, Lee P. Magnetic resonance imaging of the hand in systemic sclerosis. J Rheumatol. 2009;36(5):961–4.

52. Schanz S, Henes J, Ulmer A, et al. Magnetic resonance imaging findings in patients with systemic scleroderma and musculoskeletal symptoms. Eur Radiol. 2013;23(1):212–21.
53. Schanz S, Fierlbeck G, Ulmer A, et al. Localized scleroderma: MR findings and clinical features. Radiology. 2011;260(3):817–24.
54. Whitlock JB, Dimberg EL, Selcen D, Rubin DI. Eosinophilic fasciitis with subjacent myositis. Muscle Nerve. 2017;56(3):525–9.
55. Fett N, Arthur M. Eosinophilic fasciitis: current concepts. Clin Dermatol. 2018;36(4):487–97.
56. Mazori DR, Femia AN, Vleugels RA. Eosinophilic fasciitis: an updated review on diagnosis and treatment. Curr Rheumatol Rep. 2017;19(12):74.
57. Adachi Y, Mizutani Y, Shu E, et al. Eosinophilic fasciitis associated with myositis. Case Rep Dermatol. 2015;7(1):79–83.
58. Chaudhry AA, Baker KS, Gould ES, Gupta R. Necrotizing fasciitis and its mimics: what radiologists need to know. AJR Am J Roentgenol. 2015;204(1):128–39.
59. Finanger EL, Russman B, Forbes SC, Rooney WD, Walter GA, Vandenborne K. Use of skeletal muscle MRI in diagnosis and monitoring disease progression in Duchenne muscular dystrophy. Phys Med Rehabil Clin N Am. 2012;23(1):1–10 ix.
60. Tasca G, Iannaccone E, Monforte M, et al. Muscle MRI in Becker muscular dystrophy. Neuromuscul Disord. 2012;22(Suppl 2): S100–6.
61. Sookhoo S, Mackinnon I, Bushby K, Chinnery PF, Birchall D. MRI for the demonstration of subclinical muscle involvement in muscular dystrophy. Clin Radiol. 2007;62(2):160–5.
62. Mercuri E, Talim B, Moghadaszadeh B, et al. Clinical and imaging findings in six cases of congenital muscular dystrophy with rigid spine syndrome linked to chromosome 1p (RSMD1). Neuromuscul Disord. 2002;12(7-8):631–8.
63. Marden FA, Connolly AM, Siegel MJ, Rubin DA. Compositional analysis of muscle in boys with Duchenne muscular dystrophy using MR imaging. Skelet Radiol. 2005;34(3):140–8.
64. Degardin A, Morillon D, Lacour A, Cotten A, Vermersch P, Stojkovic T. Morphologic imaging in muscular dystrophies and inflammatory myopathies. Skelet Radiol. 2010;39(12):1219–27.
65. Lamminen AE. Magnetic resonance imaging of primary skeletal muscle diseases: patterns of distribution and severity of involvement. Br J Radiol. 1990;63(756):946–50.
66. Faridian-Aragh N, Wagner KR, Leung DG, Carrino JA. Magnetic resonance imaging phenotyping of Becker muscular dystrophy. Muscle Nerve. 2014;50(6):962–7.
67. Polavarapu K, Manjunath M, Preethish-Kumar V, et al. Muscle MRI in Duchenne muscular dystrophy: evidence of a distinctive pattern. Neuromuscul Disord. 2016;26(11):768–74.
68. Sugie K, Kumazawa A, Ueno S. Sporadic inclusion body myositis presenting with Beevor's sign. Intern Med. 2015;54(21):2793–4.
69. Milisenda JC, Rico Caballero V, García AI, Tomás X, Grau JM. "Extended" Beevor's sing as a new clinical sign in sporadic inclusion body myositis. Med Clin (Barc). 2017;148(8):e43.
70. Kornblum C, Lutterbey G, Bogdanow M, et al. Distinct neuromuscular phenotypes in myotonic dystrophy types 1 and 2: a whole-body highfield MRI study. J Neurol. 2006;253(6):753–61.
71. Kornblum C, Lutterbey GG, Czermin B, et al. Whole-body highfield MRI shows no skeletal muscle degeneration in young patients with recessive myotonia congenita. Acta Neurol Scand. 2010;121(2):131–5.
72. Kan HE, Klomp DWJ, Wohlgemuth M, et al. Only fat infiltrated muscles in resting lower leg of FSHD patients show disturbed energy metabolism. NMR Biomed. 2010;23(6):563–8.
73. Kesper K, Kornblum C, Reimann J, Lutterbey G, Schröder R, Wattjes MP. Pattern of skeletal muscle involvement in primary dysferlinopathies: a whole-body 3.0-T magnetic resonance imaging study. Acta Neurol Scand. 2009;120(2):111–8.
74. Sarkozy A, Deschauer M, Carlier RY, et al. Muscle MRI findings in limb girdle muscular dystrophy type 2L. Neuromuscul Disord. 2012;22(Suppl 2):S122–9.
75. Mercuri E, Bushby K, Ricci E, et al. Muscle MRI findings in patients with limb girdle muscular dystrophy with calpain 3 deficiency (LGMD2A) and early contractures. Neuromuscul Disord. 2005;15(2):164–71.
76. Fischer D, Walter MC, Kesper K, et al. Diagnostic value of muscle MRI in differentiating LGMD2I from other LGMDs. J Neurol. 2005;252(5):538–47.
77. Bönnemann CG, Brockmann K, Hanefeld F. Muscle ultrasound in Bethlem myopathy. Neuropediatrics. 2003;34(6):335–6.
78. Mercuri E, Lampe A, Allsop J, et al. Muscle MRI in Ullrich congenital muscular dystrophy and Bethlem myopathy. Neuromuscul Disord. 2005;15(4):303–10.
79. Filli L, Winklhofer S, Andreisek G, Del Grande F. Imaging of myopathies. Radiol Clin N Am. 2017;55(5):1055–70.
80. Fischer D, Wattjes MP. MRI in muscle dystrophies and primary myopathies. In: Weber MA, editor. Magnetic resonance imaging of the skeletal musculature. Berlin: Springer-Verlag; 2013. p. 241–4.
81. Quijano-Roy S, Carlier RY, Fischer D. Muscle imaging in congenital myopathies. Semin Pediatr Neurol. 2011;18(4):221–9.
82. Jungbluth H, Davis MR, Müller C, et al. Magnetic resonance imaging of muscle in congenital myopathies associated with RYR1 mutations. Neuromuscul Disord. 2004;14(12):785–90.
83. Klein A, Jungbluth H, Clement E, et al. Muscle magnetic resonance imaging in congenital myopathies due to ryanodine receptor type 1 gene mutations. Arch Neurol. 2011;68(9):1171–9.
84. van der Ploeg AT, Clemens PR, Corzo D, et al. A randomized study of alglucosidase alfa in late-onset Pompe's disease. N Engl J Med. 2010;362(15):1396–406.
85. Del Gaizo A, Banerjee S, Terk M. Adult onset glycogen storage disease type II (adult onset Pompe disease): report and magnetic resonance images of two cases. Skelet Radiol. 2009;38(12):1205–8.
86. Pichiecchio A, Uggetti C, Ravaglia S, et al. Muscle MRI in adult-onset acid maltase deficiency. Neuromuscul Disord. 2004;14(1): 51–5.
87. Carlier R-Y, Laforet P, Wary C, et al. Whole-body muscle MRI in 20 patients suffering from late onset Pompe disease: involvement patterns. Neuromuscul Disord. 2011;21(11):791–9.
88. Argov Z, Löfberg M, Arnold DL. Insights into muscle diseases gained by phosphorus magnetic resonance spectroscopy. Muscle Nerve. 2000;23(9):1316–34.
89. Witting N, Duno M, Piraud M, Vissing J. Severe axial myopathy in McArdle disease. JAMA Neurol. 2014;71(1):88–90.
90. Jurkatt-Rott K, Weber MA. Lehmann-horn F. MRI in muscle channelopathies. In: Weber MA, editor. Magnetic resonance imaging of the skeletal musculature. Berlin: Springer-Verlag; 2013. p. 271–88.
91. Amarteifio E, Nagel AM, Weber M-A, Jurkat-Rott K, Lehmann-Horn F. Hyperkalemic periodic paralysis and permanent weakness: 3-T MR imaging depicts intracellular 23Na overload—initial results. Radiology. 2012;264(1):154–63.
92. Tomasová Studynková J, Charvát F, Jarosová K, Vencovsky J. The role of MRI in the assessment of polymyositis and dermatomyositis. Rheumatology (Oxford). 2007;46(7):1174–9.